UNIVERSIDADE TECNOLÓGICA FEDERAL DO PARANÁ

MATEUS DEBIASI

EXPERIMENTAL EVALUATION OF CUTTINGS DISPLACEMENT BY THE DRILL BIT-DRILL STRING ASSEMBLY IN A HORIZONTAL WELL

CURITIBA

2021

MATEUS DEBIASI

EXPERIMENTAL EVALUATION OF CUTTINGS DISPLACEMENT BY THE DRILL BIT-DRILL STRING ASSEMBLY IN A HORIZONTAL WELL

AVALIAÇÃO EXPERIMENTAL DO DESLOCAMENTO DE CASCALHOS PELO CONJUNTO COLUNA-BROCA EM UM POÇO HORIZONTAL

MSc thesis presented to the Postgraduate Programme in Mechanical and Materials Engineering from the Universidade Tecnológica Federal do Paraná (UTFPR), as partial fulfilment of the requirements for the degree of Master of Engineering.
Supervisor: Prof. Cezar Otaviano Ribeiro Negrão, Ph.D.

CURITIBA

2021

Ministério da Educação
Universidade Tecnológica Federal do Paraná
Campus Curitiba

MATEUS DEBIASI

EXPERIMENTAL EVALUATION OF CUTTINGS DISPLACEMENT BY THE DRILL BIT-DRILL STRING ASSEMBLY IN A HORIZONTAL WELL

Trabalho de pesquisa de mestrado apresentado como requisito para obtenção do título de Mestre Em Engenharia da Universidade Tecnológica Federal do Paraná (UTFPR). Área de concentração: Engenharia Térmica.

Data de aprovação: 29 de Novembro de 2021

Prof Cezar Otaviano Ribeiro Negrao, Doutorado - Universidade Tecnológica Federal do Paraná

Prof Erick De Moraes Franklin, Doutorado - Universidade Estadual de Campinas (Unicamp)

Prof Silvio Luiz De Mello Junqueira, Doutorado - Universidade Tecnológica Federal do Paraná

Documento gerado pelo Sistema Acadêmico da UTFPR a partir dos dados da Ata de Defesa em 29/11/2021.

ACKNOWLEDGEMENTS

Firstly, I thank God for the opportunities that were placed in my path, as well for my family and friends.

To my family, my parents Aulemir Debiasi and Marcelina Mezzomo Debiasi, and my fiancée Roberta Zanella Puchale, for all the love and support. They made it possible for me to keep going despite the adversities.

To my great friend that the university and industry brought to me, Sandro Trindade, who believed in me and lead me in this direction.

To my supervisor and co-supervisor, Cezar O. R. Negrão and Nezia de Rosso, for opening the doors and guiding me through the mastering degree.

To all the students that were part of the TADEU work group, especially Julio Abdala, whom turned out to be a dear friend.

Finally, for all the friends that I made during the time I was in CERNN.

RESUMO

Não apenas a produção de petróleo, mas também a profundidade dos poços tem aumentado com o passar dos anos no Brasil. Como consequência, novas técnicas e tecnologias são requeridas pela indústria para extrair o petróleo de alta qualidade que é encontrado na região do pré-sal. Os poços podem ser verticais, quando o reservatório está localizado logo abaixo da posição do poço, ou direcionais, quando um ângulo de desvio é necessário para alcançar o reservatório. Considerando um poço horizontal, quando há um ângulo de 90 graus em relação a vertical, cascalhos provenientes da formação rochosa depositam-se na parte inferior do poço, criando assim um leito de cascalhos. Durante o processo de perfuração, a remoção da coluna de dentro do poço é requerida. A interação do conjunto coluna/broca com o leito de cascalhos pode aumentar significativamente o arrasto ou até aprisionar a coluna. O objetivo deste trabalho é estudar as interações entre o conjunto coluna/broca e o leito de cascalhos utilizando um aparato experimental desenvolvido para representar a situação descrita. Um aparato experimental foi desenvolvido, no qual é possível controlar o deslocamento axial e rotação da coluna, definir diferentes alturas de leitos com esferas de vidro (2,6 kg/cm³) de 3 mm de diâmetro e utilizar diferentes fluidos. O aparato registra cargas arrasto enquanto os parâmetros que foram variados são: velocidade de deslocamento em 1 e 10 cm/s, velocidade de rotação em 0 e 25 rpm, altura de leito de cascalhos em 23,6%, 35,7%, 50% e 64,3% da altura total do poço e fluidos com duas viscosidades e densidades, 1cP e 1 g/cm³ e 65 cP e 1,2 g/cm³. Observou-se que a coluna ficou presa para velocidade de 1 cm/s em um leito com altura de 50% ou maior, sem rotação e com fluido de viscosidade 1 cP. Entretanto, a formação do plugue foi evitada com a rotação da coluna ou com maior velocidade de deslocamento. Avaliando os resultados, observou-se que é possível definir uma região para o número crítico de Shields. Este número é o limite para qual valores acima dele os cascalhos são carreados pelo escoamento, enquanto para valores abaixo dele o escoamento não carreia as partículas.

Palavras-chave: Torque e arrasto; Leito de cascalhos; coluna/broca de perfuração.

ABSTRACT

Not only the oil production but also the well depths have been increasing over the years in Brazil. As a consequence, new techniques and technologies have been required by the industry in order to be able to extract the high-quality oil that has been found in the pre-salt region. The wells are usually vertical, when the oil reservoir is located right under the well position, or directional, when a deviation angle is required to reach the reservoir. Considering a horizontal well, when the deviation angle is at 90 degrees from the vertical, cuttings from the rock formation deposit on the bottom of the hole, creating a cuttings bed. The removal of the drill string from the well causes interactions between the bottom hole assembly (BHA) and the cuttings bed which may increase significantly the drag loads or even hold the pipe. The objective of this work is to study the interactions between the drill string/bit set and the cuttings bed using an experimental rig developed to represent the described situation. It was developed an experimental rig, in which it is possible to control the axial displacement and rotation of the column, set different cuttings bed heights with 3 mm diameter glass spheres (2.6 kg/cm³) and use different fluids. The apparatus registers drag loads while the parameters that were varied are: displacement speed at 1 and 10 cm/s, rotational speed at 0 and 25 rpm, cuttings bed height at 23.6%, 35.7% and 50% and 64.3% of the total well height and fluid with two viscosities and densities, 1 cP and 1 g/cm³ and 65 cP and 1.2 g/cm³. It was observed that the column got stuck for 1 cm/s displacement speed at a 50% or higher cuttings bed height, without rotation and fluid viscosity 1 cP. However, the plug formation was avoided when the column rotates or at higher displacement speed. Evaluating the results, it was observed that it is possible to define a region for a critical Shields number. This number is the limit in which values above it the cuttings are carried by the fluid flow, while for values under it the fluid does not carry the particles.

Key words: Torque and Drag, Cuttings bed, Drill Pipe/Bit.

LIST OF FIGURES

LIST OF TABLES

LIST OF ABBREVIATION AND ACRONYMS

BHA	Bottom hole assembly
ROP	Rate of penetration
T&D	Torque and drag
WOB	Weight on bit

NOMENCLATURE

Roman letters and symbols

U_c	Axial displacement speed of the column	[m/s]
h	Cuttings bed height	[m]
d_c	Column diameter	[m]
F_d	Drag force	[N]
A_{db}	Drill bit area	[m²]
V_{ae}	Effective annular velocity	[m/s]
Q	Fluid flow	[m³/s]
h_f	Fluid height	[m]
U_f	Fluid velocity	[m/s]
g	Gravity	[m]
S_h	Hole perimeter	[m]
D_{hyd}	Hydraulic diameter	[m²]
A_a	Open area	[m²]
d_p	Particle diameter	[m]
S_i	Perimeter above the cuttings bed	[m]
S_c	Pipe perimeter	[m]
r_c	Radius of the column	[m]
r_{db}	Radius of the drill bit	[m]
r_w	Radius of the wellbore	[m]
T	Torque	[N.m]
X	Well and pipe diameter ratio	[m]
d_w	Wellbore diameter	[m]

Greek letters

μ_f	Fluid viscosity	[N.s/m²]
ρ_f	Fluid density	[kg/m³]
Ω	Rotational speed	[rpm]
$\dot{\gamma}$	Shear rate	[1/s]
ρ_p	Particle density	[kg/m³]

Non-dimensional parameters

K	Clinging fator	-

Re	Reynolds number	-
θ	Shields number	-

Subscripts

$()_c$	Column
$()_d$	Drag
$()_{db}$	Drill bit
$()_{ae}$	Effective annular
$()_f$	Fluid
$()_h$	Hole
$()_{hyd}$	Hydraulic
$()_a$	Open
$()_p$	Particle
$()_w$	Wellbore

CONTENTS

1 INTRODUCTION

Despite being located in post- or pre-salt regions, oil in Brazil is mainly produced offshore. In comparison to post-salt exploitation, the pre-salt reservoirs require fewer wells. While in 1984 4,108 post-salt wells produced 500 thousand barrels a day, nowadays only 77 pre-salt wells have produced 1.5 million. This productivity increase is due to the development of new techniques applied to ultra-deep-water drilling and the large amount of oil found in the pre-salt reservoirs. Additionally, the oil from the pre-salt has high quality and high commercial value. However, drilling deeper pre-salt wells in ultra-deep-waters is quite costly. The cost of operation per day is in the order of one million dollars (Petrobras 2019).

The production in the pre-salt region must be highly efficient to reduce the operation time so as to provide a competitive oil price. An alternative to reduce the exploitation cost is the process optimization, which may reduce significantly the time required, ensuring a better selling price and high competitiveness. Even though the production nowadays is significantly efficient, challenges in drilling technology, knowledge and personnel capability are still faced (Petrobras 2014; Petrobras 2019).

It is quite common to drill wells right above the reservoir, resulting in vertical wells, as shown in Figure 1 (a). However, sometimes it is not possible to drill vertical wells due to geographic issues. A solution to this problem is to drill directional wells, in which the well deviates from the vertical in angles that varies from 0 to 90 degrees, as depicted in Figure 1 (b). An extreme deviation of 90 degrees leads to a horizontal well (see Figure 1 (c)). Horizontal wells are also used to enlarge the well-reservoir contact area for shallow reservoir in order to increase oil production (Petrobras 2015a).

Figure 1. Different drilling methods. (a) Vertical well. (b) Directional well. (c) Horizontal well.

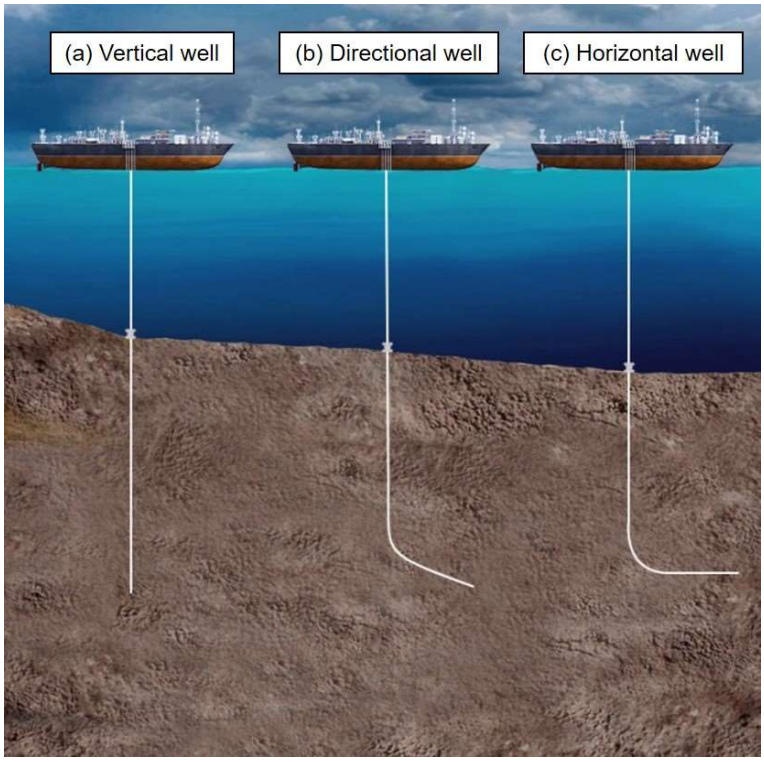

Source: Petrobras (2015a)

Drilling occurs due to the drill bit interactions with the rock formation which is obtained by applying axial force to the drill string against the rock and torque to the drill string. The drill bit shears and breaks the rock into small fragments known as cuttings (Petrobras 2015b). While drilling directional wells, the cuttings may settle down forming a bed that increases with the deviation angle (Sifferman and Becker 1997; Wang et al. 2017). A good drilling process requires the well to be cleaned constantly. To clean the well the drilling fluid is injected through the drill column to reach the drill bit and to carry the cuttings to the surface. When the fluid flow rate is not high enough to erode the cuttings bed, the bed height increases creating a series of drawbacks to the drilling process (Costa 2006). Common related problems are: reduction of rate-of-penetration (ROP), weight-on-bit (WOB) and increase of torque and drag (T&D) loads (Rasi 1994).

The T&D increase when the column is removed from the wellbore and the cuttings bed is displaced by the drill bit and by the bottom hole assembly (BHA) elements, rising the cuttings volume behind the elements. The cuttings bed displacement by the drill bit-bottom hole assembly is illustrated in Figure 2. Considering the initial condition shown in Figure 2 (a), two scenarios may occur during the removal of the drill string. In the first, as depicted in Figure 2 (b), a constant volume hill is formed

on the elements of the BHA, as the volume of cuttings displaced by the elements equals the amount carried by the fluid flow. In the second, shown in Figure 2 (c), a plug is formed as the volume of displaced cuttings exceeds the amount conveyed by the fluid. Considering the plug length increases continuously, the column may get stuck due to excessive drag force (Rasi 1994).

Figure 2. Displacement of a cuttings bed by the drill bit-drill string assembly in a horizontal well. (a) initial state. (b) formation of a constant volume hill. (c) formation of a plug. The red arrow indicates the drill string displacement direction.

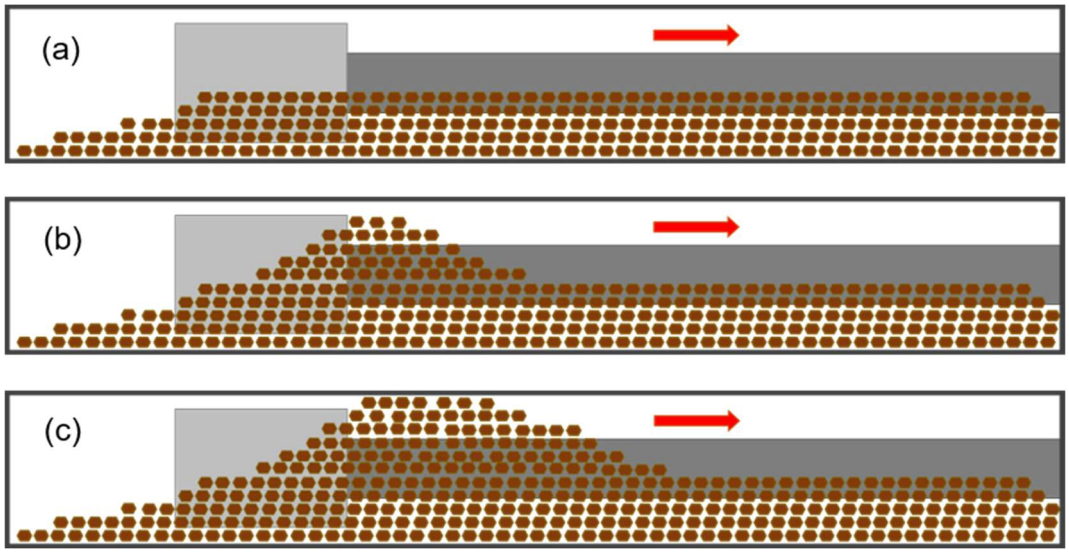

Source: Author (2021)

The torque is defined as the moment required to rotate the pipe and the drag is the force needed to move the pipe up or down in the hole. There are two approaches to model T&D, named the soft- and stiff-string models. The main difference between them is that the soft-string approach does not consider the bending stiffness (Mitchell et al. 2007), while the stiff-string model considers the pipe deflection due to axial forces that occurs in pipe compression and due to the well-path trajectory (Johancsik et al. 1984). Stiff-string models are more complex in comparison to soft-string ones, since the wellbore profile is really difficult to recognize. A limitation of the T&D models is the use of general friction factor that accounts for all friction forces between the well bore and the column elements, which must be fit to experimental data. Both soft- and stiff-string T&D models do not consider the cuttings bed and BHA interactions which are embodied as one of the friction forces that compose the well bore and column element interactions. Depending on how the cuttings behave during the removal of the drill

string from the well bore the drag force can be high enough to cause the stuck pipe scenario, which are not considered in modeling. In order to fulfill this gap in the literature, an experimental rig representing a horizontal well was built in laboratory scale so as to study the interactions between drill string/bit set and cuttings bed during the pipe removal.

1.1 General objective

The current work's objective is to analyze experimentally the interactions between drill string/bit set and cuttings bed while the pipe is pulled out of the well. The experiment was performed using a laboratory scale representation of a horizontal well. In order to better understand what would avoid or cause the undesirable stuck pipe cuttings bed heights, column axial displacement speed and column rotation were varied. This is an important contribution since the phenomenon that take place between the BHA and cuttings bed is not considered in modeling of drag forces.

2 LITERATURE REVIEW

This chapter presents a literature review that is divided into three sections: i) mathematical T&D models, expressing the general use of friction factor; ii) experimental works that dealt with similar conditions as the one studied in the current study; and iii) granular media, in order to better understand cuttings displacement during the column movement.

2.1 Mathematical models

The first work related to T&D modeling was conducted by Johancsik et al. (1984), which observed that T&D loads are a result of sliding friction. Trying to foresee the T&D loads, the sliding friction was computed by multiplying a friction factor coefficient by the sidewall contact area. The authors stated that friction coefficients for seawater-based mud systems in directional wells are in the range of 0.25 to 0.40. Johancsik's et al. (1984) model considers that the only cause of T&D is the sliding friction, influenced by the normal force and the friction coefficient.

Mitchell et al. (2007) worked on Johancsik's model, using Sheppard et al. (1987) equation, and also verified that it fits very well to the field data. They considered a soft-string model, since it neglects the stiffness of the column. The study provided an approximate formula to evaluate the effects of wellbore curvature and torsion. Their T&D model formulation solves the problems related to the column-wellbore contact by considering that the drill string trajectory coincides with the wellbore path. According to the authors, the friction coefficient required to match the drag force calculated with the field data is significantly different from the one required to match the torque. In order to fit the torque, they considered shear forces due to the rotating drill string tendency to climb the wellbore wall. The main drawback of this T&D model is the assumption of the minimum curvature wellbore trajectory. This method does not consider some contact and axial loads, underestimating T&D loads. The work of Aadnoy et al. (2010) presented a new friction model that is applied for straight sections, drop-off bends, build-up bends, side bends or a combination of them. It is a soft-string model aiming at providing a simple tool to model and to study the well friction by separating gravitational and friction effects.

A newer and simpler approach for stiff-string calculation was introduced by Mirhaj et al. (2016). Their goal was to determine when stiff-string models are

applicable. A constant curvature trajectory with a continuous contact between wellbore wall and pipe is considered. A critical limit of 1% between the axial force computed by the soft-string in comparison to stiff-string model was defined. For differences smaller than or equal to the critical limit, the soft-string model is considered suitable. It is worth mentioning that the soft-string model worked very well for the majority of T&D cases that were studied by the authors and that the soft-string model could be used in most part of the well, except for the high-tortuous regions and stiffer pipes, such as the BHA. For differences higher than 1%, the stiff-string model should be used.

It is possible to verify the usage of a general friction factor by analyzing the T&D modeling works conducted over the years. All works related to the matter use a friction factor, although none consider the interactions between the BHA and the cuttings bed.

2.2 Experimental works

Only few experimental works related to the current study were found in the literature. The first one was conducted by Rasi (1994). He stated that for horizontal wells the elements of the BHA tend to plow the cuttings bed during the axial displacement. The problem he worked on is shown in Figure 3. Through a series of laboratory experiments, he determined a cuttings bed height threshold for plug formation. The pipe may get stuck if the cuttings bed is higher than a critical height.

Figure 3. Well path caracterization. The well's path contains wall enlargements and closures, as well as cuttings bed on the horizontal portion of the hole.

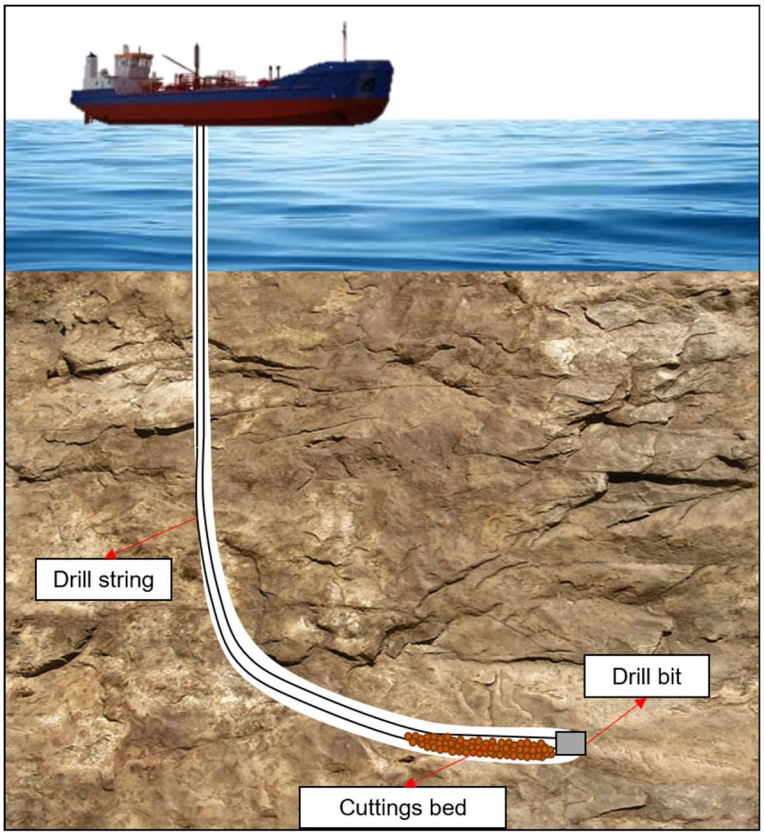

Source: Adapted from Rasi (1994)

He also used several models of BHA that were pulled inside transparent pipes partially filled with cuttings bed. He varied the pipe size, bit cross-sectional area and shape, collar length and outside diameter, initial cuttings bed height, type of cuttings and wellbore inclination. Two main conditions were observed with these experiments. In the first, the pipe displacement created a hill of cuttings that grew in the beginning of the movement and soon stopped growing, maintaining a continuous length without increasing the overpull, as illustrated in Figure 4 (a). This condition was found when the cross-sectional area of the largest element of the BHA was smaller than the open area above the cuttings bed. In the second, the hill increased continuously with the pipe motion rising the overpull and sometimes exceeding pulling capabilities, as shown in Figure 4 (b). In this case, the BHA elements were larger than the open area above the cuttings bed.

Figure 4. Displacement of BHA on a cuttings bed, as observed by Rasi (1994) (adapted). (a) a hill is formed with constant volume. (b) a plug is formed, closing the annular space. The red arrow indicates the drill string displacement direction.

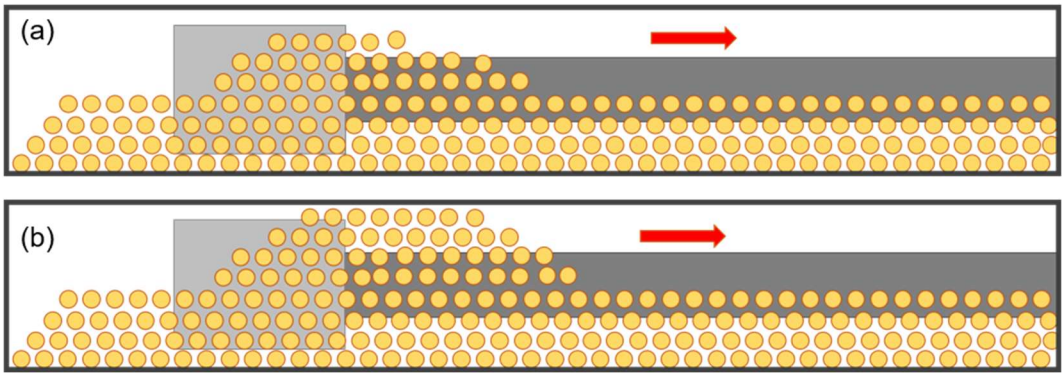

Source: Author (2021)

With the goal of fulfilling the gaps of Rasi's (1994) work, Peliano (2018) built up an experimental rig to analyze the T&D for drill strings partially immersed by cuttings bed. The evaluation was performed by considering four cuttings bed heights, two drill bit models, glass spheres as cuttings and water as fluid. To study the influence of cuttings bed height, four heights were defined: 33, 50, 70 and 90 mm from the bottom of a 140 mm-plexiglass pipe. Peliano (2018) has also evaluated the effect of the axial displacement speed by changing it from 10 to 50 cm/s. He observed that the increase of the cuttings bed height favored the plug formation. It is also known from Rasi's (1994) work that the increase of the drill bit cross-sectional area impaired the cuttings flow during the pipe displacement resulting in plug formation, which was also observed by Peliano (2018). Nevertheless, he observed three conditions during the performed tests: i) the cuttings reached the upper side of the pipe, forming a plug that grew continuously in length up to a point the pipe got stuck; ii) the plug was formed but did not grew continuously; iii) a hill was formed but did not grew during the pipe displacement.

The work of Knesebeck (2018) used the Peliano's (2018) experimental rig to check for the influence of pipe rotation during the axial pipe displacement. He fixed the axial displacement speed in 30 cm/s, used three cuttings bed height: 33, 50 and 70 mm from the bottom of a 140 mm wellbore, and four different rotational speeds: 0, 50, 100 and 150 rpm. Despite the pipe getting stuck for every condition he tested, rotation had a negative influence. Not only the plug was formed sooner but also the pipe got

stuck earlier when rotation was applied. However, the rotational speed was not significant, since the results for 50, 100 and 150 rpm were very similar.

It can be concluded from the reviewed works that the smaller open areas above the cuttings bed the higher the chances of plug formation and consequently, of getting the pipe stuck. Additionally, the open area above the cuttings bed should be larger than the BHA elements area to avoid plug formation. Moreover, the pipe rotational speed for the author's condition does not have a significant influence on the results, however, the rotation itself have a negative contribution anticipating the plug formation in comparison to non-rotating scenarios.

2.3 Cuttings bed and granular media

Trying to understand the complex phenomena that occurs during the displacement of the column/drill bit on a cuttings bed, a literature review about the displacement of granular media was conducted.

Most works related to cuttings displacement are concerned with well cleaning process. A full-scale wellbore simulator at low pressure and temperature was used by Nazari et al. (2010), in which they observed that increasing the hole angle increased the hydraulic need for hole cleaning. The authors observed that the transport of smaller cuttings is more difficult and that annular cuttings concentration and bed height are two hole cleaning parameters that need to be monitored. Zhou (2008) also observed that the smaller the cuttings the higher the flow velocity needed to transport them. The decrease in flow velocity also decreased the cuttings transport capability. Based on the results, he stated that the cuttings volume at the annulus was sensitive to the liquid flow rate.

Wiktorski et al. (2018) used an experimental rig that consisted of a glass pipe with a plexiglass pipe inside to represent the wellbore and drill string, respectively. Glass pallets were used as grains and water as fluid. Using a flow rate in which the local liquid velocity is above the critical flow velocity resulted in separate particle dunes. By increasing the flow, a homogeneous suspension of particles was created. According to the authors the bed height was a function of flow rate. Cúñez and Franklin (2019) performed a laboratory experimental work to study the liquid-solid fluidized beds in a narrow vertical tube. A water reservoir, a heat exchanger, a centrifugal pump, a flow meter, a flow homogenizer, a one-inch tube and a return line were used as the

experimental setup. The authors observed granular plugs and voids occupying the hole tube, and these plugs depended strongly on the water flow, not on the initial height.

Allen and Kudrolli (2018) developed an apparatus of a cylindrical container, with a conical top plate that could be rotated with a previous set frequency. This rotation would apply to the fluid a uniform shear stress, so it would be possible to understand the behavior of a bed of monodisperse spherical grains to the fluid flow. The test start point was a freshly sedimented bed in which, when vibration was applied the packings compacted rapidly. The deep shear-induced relation of the bed caused the bed armoring, that was the reason for the volume fraction increase. The authors demonstrated that to erode the bed, a significantly higher shear stress was needed after the application of a sub-critical shear.

Considering that the cuttings bed is a granular medium since it is formed by the setting of cuttings prevenient from the drilling process, one can consider the drill bit/string set a rigid body that is moving through the medium. Hamm et al. (2011) used an apparatus that consisted of a rigid finger entering a granular medium, they observed that the particles affected by the body are within a region according to the penetration depth. Which consists in rest for the particles out of this range. The particles that are affected can be divided in two shear bands, first by the movement of the rigid body and later the second that sticks to the moving particles and starts flowing. (Tordesillas et al. 2014) also studied the penetration of a rigid body in granular medium, they observed the rearrangement of the particles, which creates contact circles and force chains. Thus, the rigid body entering the granular medium creates force chains between the particles by its movement.

Although the particle displacement studies found in literature are not for removing a drill string from a well, it was observed that small cuttings are more difficult to be carried by the fluid and that the fluid velocity and shear stress have an important role in cuttings transportation. Moreover, the more compact the cuttings bed the higher is the shear stress required to erode the bed. However, once a rigid body is moved through a granular medium the particle behavior changes moving the shear bands creating chain connections between the particles.

2.4 Synthesis

In this chapter, a literature review was conducted. Two approaches are usually used for T&D modeling: soft- and stiff-string. The main difference between the models is that the soft-string model neglects the pipe stiffness. Additionally, the interactions between drill string/bit set and cuttings bed are not considered.

Only three experimental works, Rasi (1994), Peliano (2018) and Knesebeck (2018), were found to be directly related to the current study. Rasi (1994) was the first one to relate the drill bit open area to the amount of cuttings in the wellbore. Peliano (2018) used an experimental rig to study the influence of the axial displacement speed for two different drill bit areas and four cuttings beds heights, using glass spheres as cuttings and water as fluid. Knesebeck (2018) used the same rig to study the influence of rotation at one determined axial displacement speed.

The granular media studies dealt with the interaction of fluid flow and the media. Nonetheless, none of the mathematical models consider the interaction of the BHA on a cuttings bed. Therefore, studying the interactions between column/drill bit and cuttings bed may contribute to understand the phenomenon.

2.5 Specific objectives

A set of parameters will be varied in order to evaluate the interactions when the drill string/bit set is pulled out of the horizontal well. Such parameters are listed:

- Axial displacement speed of 1 and 10 cm/s. These displacement speeds were set since Peliano's (2018) work varied it from 10 to 50 cm/s. In this work, the influence of low displacement speed will be analyzed.
- Rotational speed of 0 and 25 rpm. In order to avoid reading noise due to excessive pipe vibration, the rotational speed was set to the small value of 25 rpm, since Knesebeck's (2018) work showed that the speed does not have significant influence on the hill or plug formation.
- Cuttings bed heights of 23.6%, 35.7% and 50% of the well’s cross-sectional area with glass spheres of 3 mm diameter and 2600 g/cm³. The works on the literature review showed that the larger the cuttings bed heights more probable is the plug formation. The maximum height used was 50% of the

well's cross-sectional area as higher values were evaluated by Peliano (2018) and Knesebeck (2018).

- Water (1 cP and 1 g/cm³) and a solution of glucose syrup (65 cP and 1.2 g/cm³) as fluids. While water is a common fluid for all the works reviewed, in the current work the influence of a higher viscosity fluid will be also investigated.

3 METHODOLOGY

The experimental rig used in the current work is now described. This experimental rig was developed to represent a horizontal well aiming to study the interactions of the column-drill bit set and cuttings bed.

3.1 Description of the experimental rig

The current experimental rig is an enhancement of the one developed by Hambrusch et al. (2017), Peliano (2018) and Knesebeck (2018). Figure 5 shows a drawing of the rig.

Figure 5. Experimental rig. (1) Plexiglass pipe that represents the well. (2) Mechanical subsystem responsible for the axial displacement and rotation. (3) Aluminum pipe representing the drill string. (4) Polypropylene drill bit model. (5) Fluid entrance.

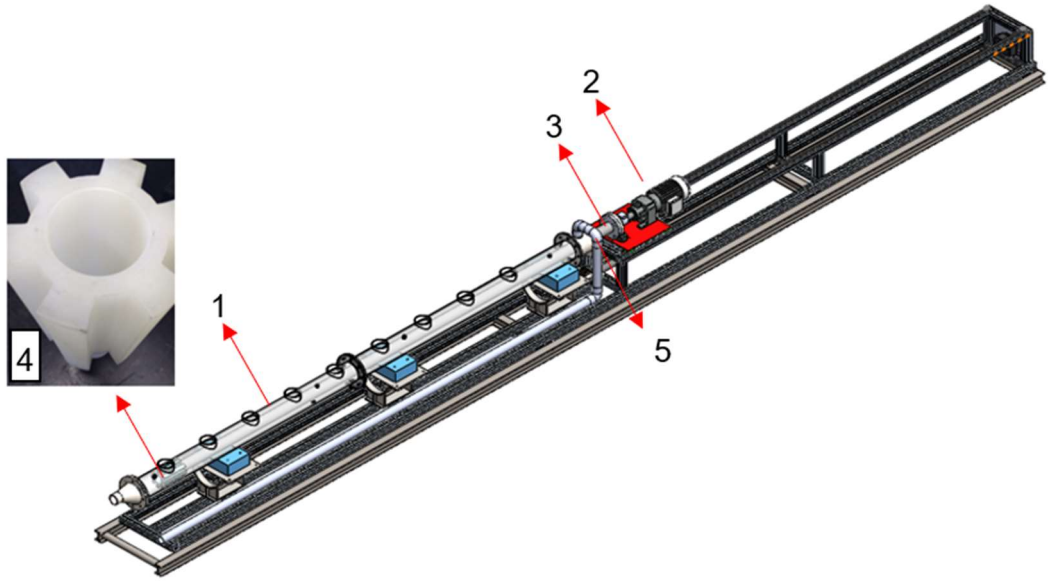

Source: Author (2021)

This experimental rig was developed to mimic the drill pipe pull out from a horizontal wellbore. The rig is composed of three main systems: the test section that represents the horizontal well; the mechanical system responsible for the column movements; and the data acquisition system that register the measurements.

The wellbore is represented by a 4 m long plexiglass pipe with a diameter of 140 mm, as indicated by the number (1) in Figure 5. A 4 m long aluminum pipe with a diameter of 76.2 mm is placed inside the wellbore to represent the drill pipe, depicted

by the number (3) in Figure 5. The drill bit is attached to the left edge of the aluminum pipe; the element (4) in Figure 5. The mechanical system (2) moves axially and rotate the column inside the wellbore. The entrance (5) is used to feed the plexiglass pipe with working fluid. The apparatus is supported by an aluminum structure that is composed of 50x50 mm commercial X profiles standing over rubber shoes that are used to level the system basis and to absorb excessive vibration.

Figure 6 shows the components of the test section that comprises the 140 mm-internal-diameter plexiglass pipe (1), the 76.2 mm-external-diameter aluminum pipe (2) and the Polypropylene drill bit model (4) attached to the end of the aluminum pipe. A total of nine four-inch opening gates (3) were assembled on the upper side of the plexiglass pipe to allow access to the cuttings bed, when closed the inner part has the same degree as the pipe, which does not influence in the pipe or cuttings displacement.

Figure 6. Test section. (1) Plexiglass pipe representing the wellbore. (2) Aluminum pipe representing the drill string. (3) Opening required to place the cuttings bed.(4) Representation of the drill bit.

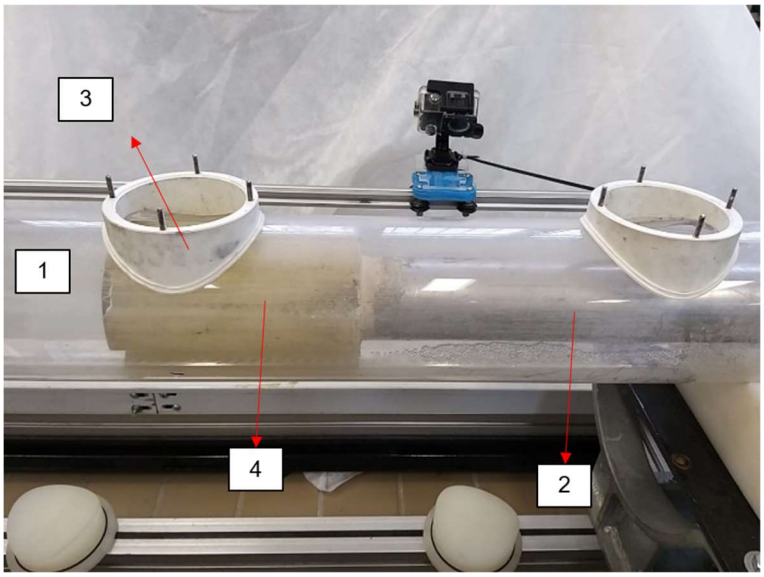

Source: Author (2021)

The drill bit model was designed to represent a drill bit with the external diameter of 130 mm with grooves of 40 mm, allowing space for fluid and cuttings to flow axially, as depicted in Figure 7.

Figure 7. Drill bit model manufactured in Polypropylene with grooves. External diameter of 130 mm.

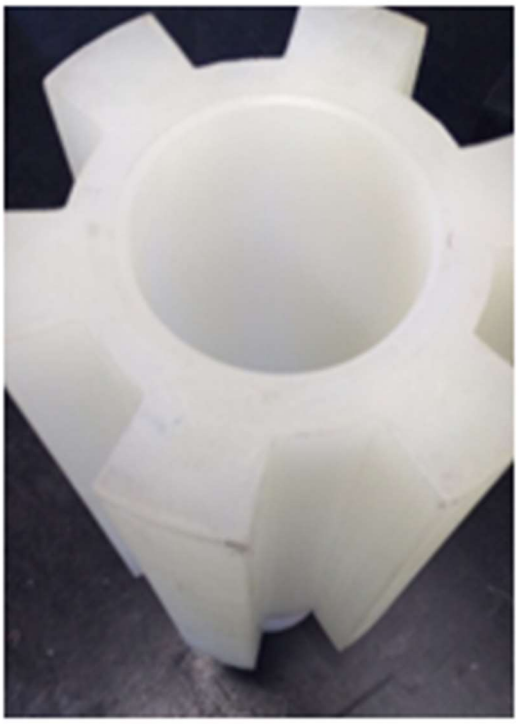

Source: Author (2021)

The components of the mechanical system are shown in Figure 8. A four-meter ball screw with 50 mm diameter (1) is driven by a servomotor (2). This servomotor - an Hiwin model FRMS752B608C, with nominal rotation of 3000 rpm and a 9.2 Transtecno reduction type CMB502 - is placed at one end of the ball screw. It is powered and controlled by the software Lightening by Hiwin. The ball screw rotation is responsible for transporting the nut at 10 mm pitch that is attached to a load cell sensor. This displacement system is responsible for the drill-pipe movement, which has a three-meter path with emergency stop buttons. As depicted in Figure 9, an electric motor (3), model SK80S/4, mounted on the plate (4) that is guided by linear guideways, is responsible for the drill-pipe rotation. The system enables controlling the axial displacement speed and the pipe rotation. The drill-pipe movement is controlled by two computer software codes: LabVIEW that enables the power of the electric motor and servo, and controls the rotation of the column, and Lightening that controls the axial displacement of the column.

Figure 8. Mechanical system. (1) Ball screw and nut responsible for the column motion. (2) Servomotor responsible for the ball screw rotation.

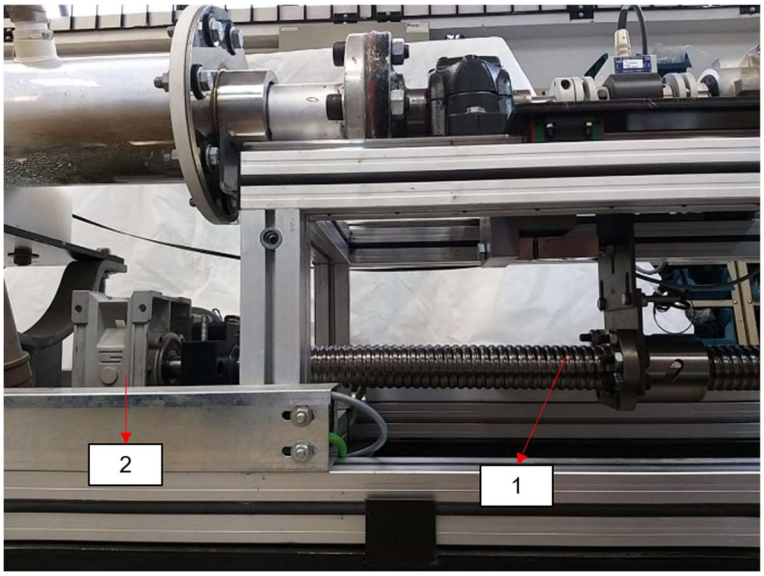

Source: Author (2021)

Figure 9. Mechanical system. (3) Motor responsible for the drill-pipe rotation. (4) Plate that supports the electric motor and slides on the guideways.

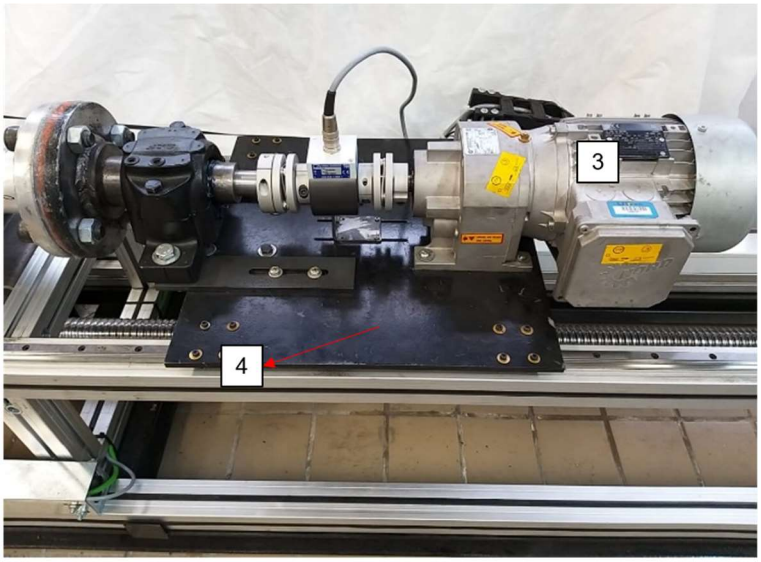

Source: Author (2021)

As shown in Figure 10, the data acquisition and control system are composed of a National chassis NI cDAQ-9188 with three slots used for the data acquisition of the traction load cell. The system communicates via LabVIEW. The traction load cell, an HBM S9M of 2000 N of nominal force, is placed underneath the plate that holds the column to measure the forces required to displace the column during its axial movement. The cell operates in a frequency of 2000 Hz at continuous reading of 4000

samples with an accuracy class of 0.02. The traction load cell is installed with cable filters and the wires are placed in different sides of the rig using a wire transformer to avoid electric noise.

Figure 10. (1) Traction load cell.

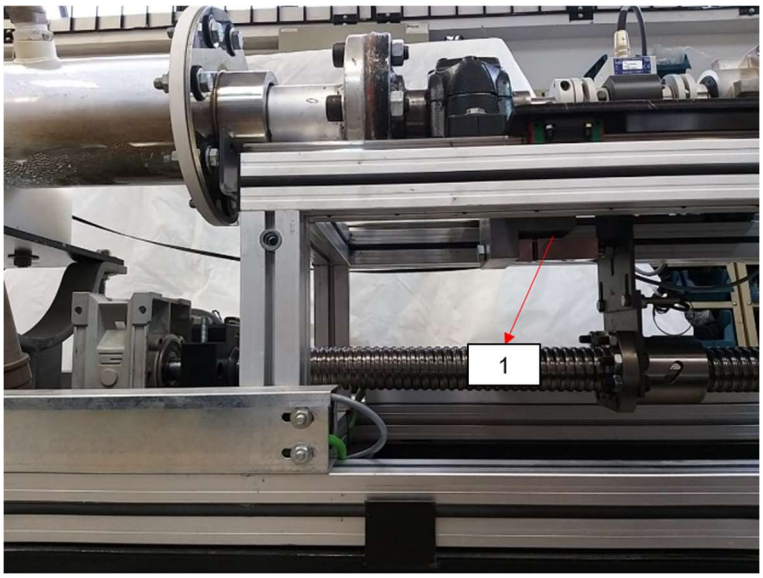

Source: Author (2021)

3.2 Uncertainties analysis

A series of measurement uncertainties may exist in experiments. The uncertainties are separated in two kinds: systematic, from the measuring systems; and random, that influence the measurement indirectly (Baratto et al. 2008; Coleman and Steele 2018). The experimental rig uncertainties are listed in Table 1.

Table 1. Systematic and random uncertainties causes

Causes	Systematic uncertainty	Random uncertainty
Traction [N]	0.4	4
Cuttings bed height [mm]	0.35	2
Rotational speed [rpm]	0.1	0.2
Displacement speed [cm/s]	0.01	0.013
Displacement length [mm]	0.5	4

Source: Author (2021)

The systematic uncertainty of each equipment was obtained from their respective manuals, while the random uncertainties were obtained from the average of a series of measurements during the tests performed. Since the objective of the current work is to analyze the drag forces, which depends on the traction load cell readings, several tests pulling the same mass without spheres were performed. These tests resulted in a random uncertainty of ±4 N. The random uncertainty of the cuttings bed height formation was also measured from a series of beds after being constructed, as well for the displacement and rotational speed and displacement length. The experimental rig's uncertainty is composed by the systematic and the random uncertainties. It implies that for every reading from removing the column from the wellbore the drag force in the tests performed have an uncertainty of ±4 N.

3.3 Test methodology

The aim of the current analysis is to investigate the sensitivity of the drag force on changes of axial motion speed, drill string rotation and the cuttings bed heights. According to field information, the column displacement speed is within the range of 10 to 22 cm/s and the rotation speed between 80 to 140 rpm.

Considering the axial speed limit of the experimental setup is 10 cm/s, the values of 1 and 10 cm/s were chosen for the tests. The lowest value enables to evaluate low displacement speeds to verify its influence on the formation of cuttings hills and plugs. Considering the vibration caused by the rotational speed is quite significant for typical field values and that the work of Knesebeck (2018) has shown that the speed of rotation does not have a significant impact on the plug formation, the rotation speed was set to 25 rpm.

The cuttings bed heights were varied to represent an almost clean well to a poor cleaned one. The 33 mm and 70 mm cuttings bed heights represent 23.6% and 50% of the well diameter, respectively. 3 mm diameter glass spheres (2600 g/cm³ density) were used to represent the cuttings. In order to verify the influence of fluid viscosity, water (1 cP) and a solution of glucose syrup (65 cP and 1.2 g/cm³) were used as working fluids.

The set of parameters that were varied during the experiments is shown in Table 2. The tests were performed by fixing three variables and changing the fourth.

The reference case is defined as water, cuttings bed height of 33 mm and axial displacement speed of 10 cm/s, without rotation.

Table 2. Test matrix

Fluid	Water		Glucose syrup sol.
Cuttings bed height [mm]	33	50	70
Axial displacement speed [cm/s]	1		10
Rotation speed [rpm]	0		25

Source: Author (2021)

3.3.1 Test procedure

The test procedure is described in Figure 11. Firstly, the column is introduced completely in the well, placed at the initial test position named as P1. Secondly, the drill string is removed from the well, travelling a 3 m distance. A cuttings bed leveling device is attached to the drill string through the last opening gate. These leveling devices, shown in Figure 12, are used to level the cuttings bed to a defined height. Three different cuttings bed heights can be chosen: 33, 50 and 70 mm, that represents 23.6%, 35.7% and 50% of the well diameter.

Figure 11. Test procedure description as a working flow

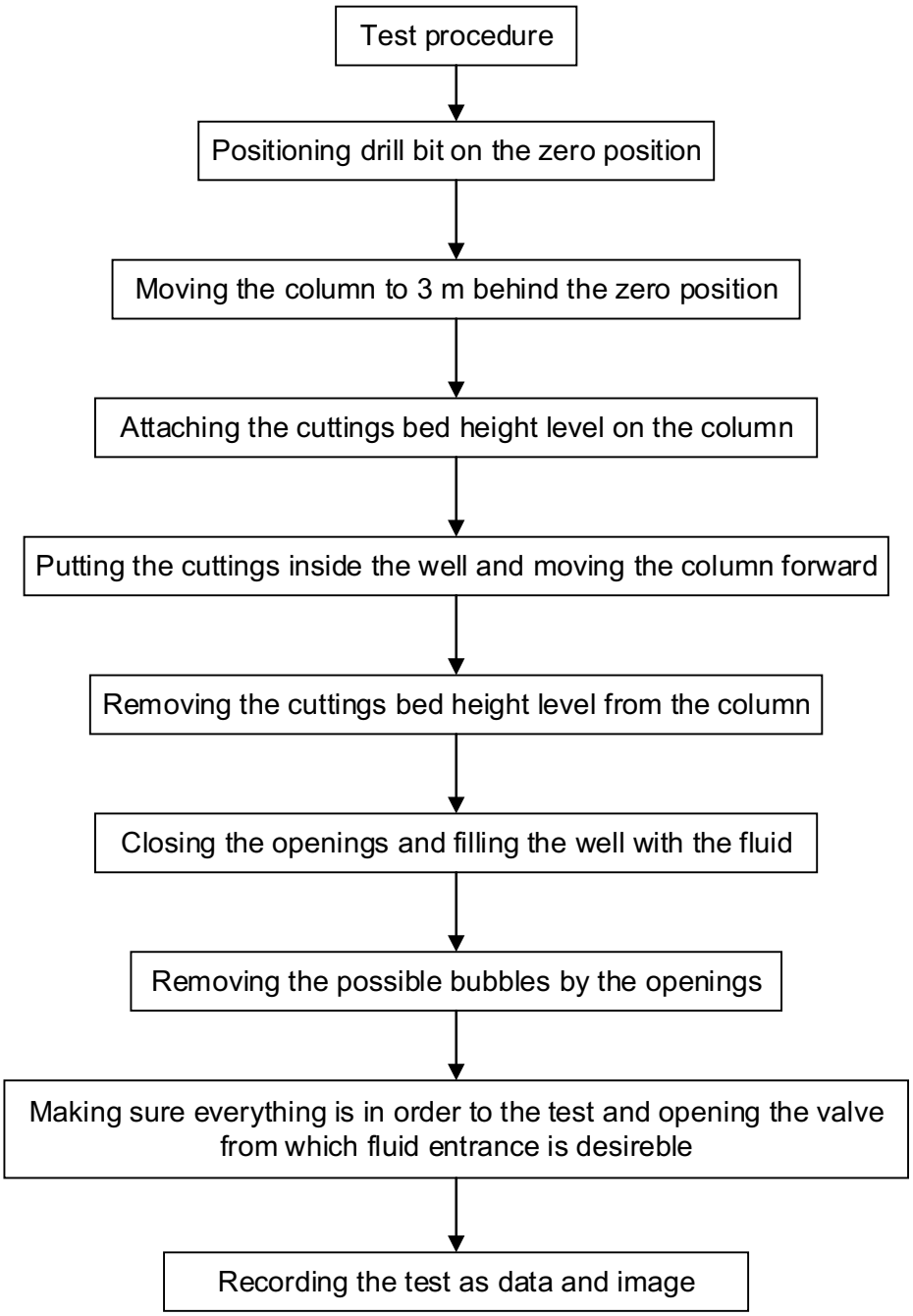

Source: Author (2021)

Figure 12. Cuttings bed leveling representation.

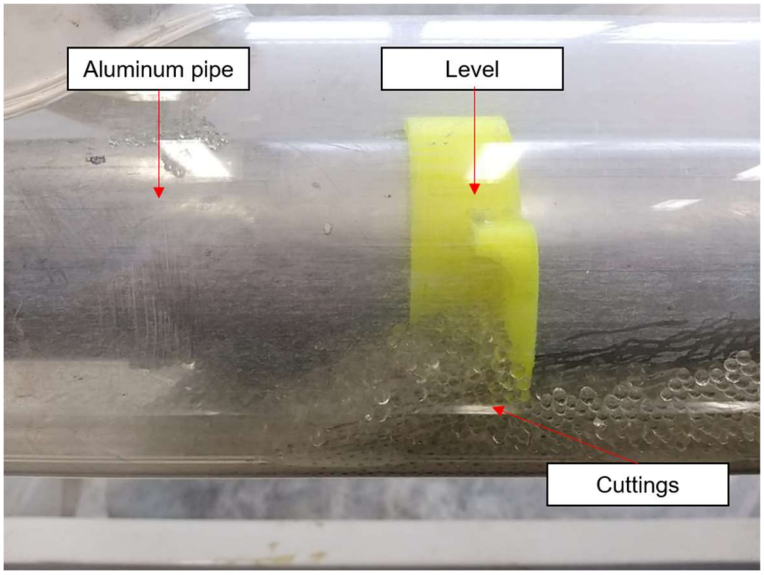

Source: Author (2021)

The cuttings are then introduced inside the well just ahead of the leveling device. The column is then moved forward leveling the cuttings bed. The process is repeated until the whole 3 m path is completely filled with cuttings on the desired level. The cuttings bed level is then removed from the column through the first opening gate. After building the cuttings bed, as shown in

Figure **13**, all the opening gates are closed. The fluid valve is then opened, allowing the fluid to fill the well by gravity. Air bubbles may remain in the well after filling it with fluid. The valves are closed and a hydraulic pump attached to a hose is used to remove the air bubbles by the openings. From this point on, the test is ready to be conducted and it is controlled only by computer software.

Figure 13. Cuttings bed of 33 mm height.

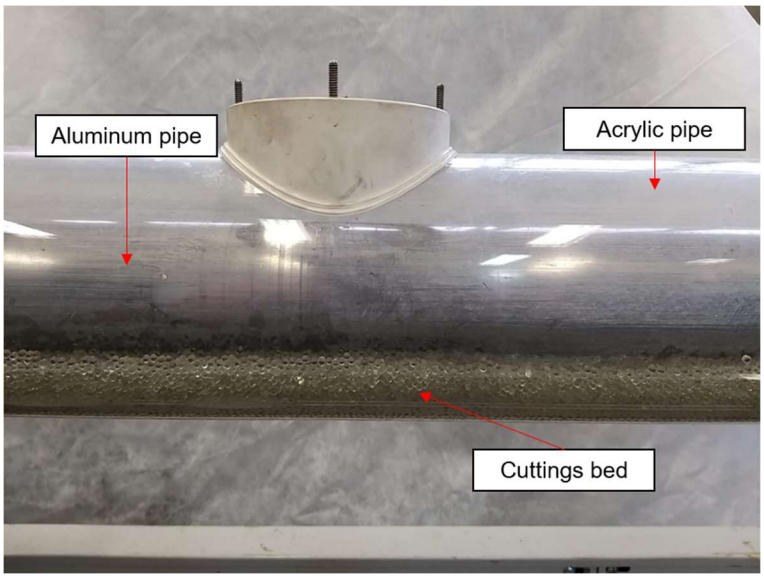

Source: Author (2021)

Using LabVIEW and Lightening software, the rotation and axial displacement speed are controlled. The load cell readings are recorded by the LabVIEW program. The user sets the desirable displacement speed, the rotational speed, enables the record button and finally, releases the drill string movement.

3.4 Reynolds number

The Reynolds number was calculated in order to verify the flow regime during the tests. The calculation was performed for both water and the glucose syrup solution. The works of Fontenot and Clark (1997), Tang et al. (2016) and Rojas et al. (2017) were used as the base for the Reynolds number calculation.

The Reynolds number (eq. 3.1) was calculated to all initial tests' conditions, both for drill bit and string. It considers the effective hydraulic diameter, eq 3.2, with the correction used by Tang et al. (2016), the effective velocity that considers the fluid flow for the drill bit or the drill string, fluid density and viscosity. During the displacement of the drill string, the fluid is dislocated at the upper part of the cuttings bed and then at the annular space between the drill bit and the well, also preferably on the upper part, due to less resistance. In figure Figure 14 and Figure 15 it is possible to see the areas

above the cuttings bed for the column and drill bit, respectively, calculated by the perimeters in eq. 3.3 to 3.5 and the open area in eq. 3.6.

Figure 14. Representation of the area computed above the cuttings bed for the column region, showing the perimeters S_c, S_i and S_h.

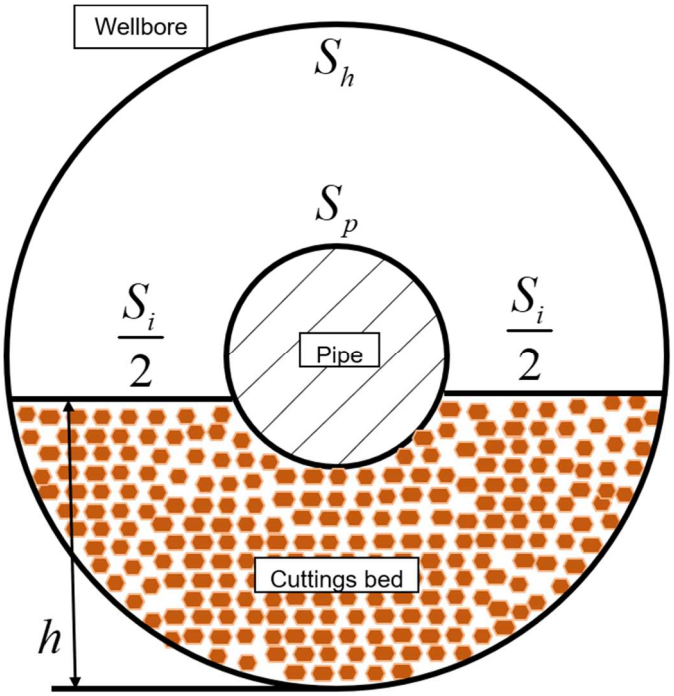

Source: Adapted from Tang et al. (2016)

Figure 15. Representation of the area calculate above the cuttings bed for the drill bit region, showing the perimeters S_{db}, S_i and S_h.

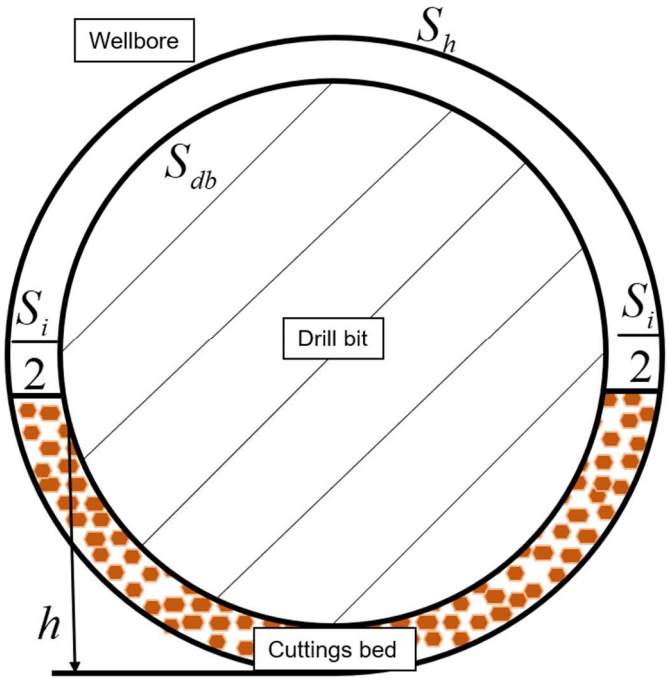

Source: Adapted from Tang et al. (2016)

- Reynolds number (Re)

$$\mathrm{Re} = \frac{D_{hyd} V_{ae} \rho_f}{\mu_f} \tag{3.1}$$

In which:

- Hydraulic diameter (D_{hyd})

$$D_{hyd} = \frac{4A_a}{S_h + S_c + S_i} \tag{3.2}$$

where:

$$S_h = d_w(\pi - \arccos(\frac{1-2h}{d_w})) \tag{3.3}$$

$$S_c = d_c(\pi - \arccos(\frac{1-2(h-X)}{d_c})) \tag{3.4}$$

$$S_i = 2\sqrt{h}(d_w - h) \tag{3.5}$$

- Open area above the cuttings bed height (A_a)

$$A_a = \pi r_w^{\,2} - \pi r_{db}^{\,2} - (\frac{r_w^{\,2}}{2} - \frac{r_{db}^{\,2}}{2})(2\arccos(\frac{r_w - h}{r_w}) - \sin(2\arccos(\frac{r_w - h}{r_w})) \quad (3.6)$$

The open area above the cuttings bed is the white portion shown in Figure 14 and Figure 15, for the drill string and drill bit regions, respectively. The wet perimeters are those in which the fluid is in contact with is the perimeter of the wellbore, S_h, the column, S_c, or the drill bit, S_{db}, and above the cuttings bed, S_i. With these perimeters it is possible to calculate the hydraulic diameter for the pipe and for the drill bit region. It is possible to observe that the flow area in the drill bit region is much smaller than its counterpart in the column region, which increases the Reynolds number.

The areas and the hydraulic diameter were calculated based on Tang's et al. (2016) work. In the current work, the effective diameter was used as the hydraulic. The reason is that the effective diameter is a correction for the hydraulic diameter considering the fluid flow for a partially immerse drill string in a cuttings bed.

- Annular effective velocity (V_{ae})

$$V_{ae} = \frac{Q}{A_a} + U_c K \quad (3.8)$$

Also, the fluid velocity used to calculate the Reynolds number is the annular effective velocity. The effective velocity is the annular fluid flow speed (for the drill bit or the drill string) that considers the fluid velocity due to the fluid flow in the annular area and adds the clinging factor multiplied by the column displacement speed. The fluid flow rate, Q in eq. 3.9, the clinging factor, K in eq. 3.10, and the open area above the drill bit or drill string are required to calculate the annular effective velocity.

- Fluid flow rate to replace the space left by the drill bit (Q)

$$Q = U_c A_{db} \quad (3.9)$$

The fluid flow for this part of the calculation is the one caused by the pipe displacement. While the pipe is removed from the well, the volume that the drill bit was occupying must be filled with the fluid.

- Clinging factor (K)

$$K = \frac{X^2 - 1 - 2\ln(X)}{2(X^2 - 1)\ln(X)} \tag{3.10}$$

This factor is used due to the friction that exists between the fluid and the pipe. While the pipe is displaced there is an amount of fluid that is attached to the pipe. As depicted in Figure 16, it is possible to verify that when the pipe is displaced in the direction of U_c there is a portion of fluid that is around the pipe that flow in the same direction, even when the flow, Q, is in the opposite direction.

Figure 16. Representation of clinging. The layer of fluid attached to column is dragged in the opposite direction of the fluid flow.

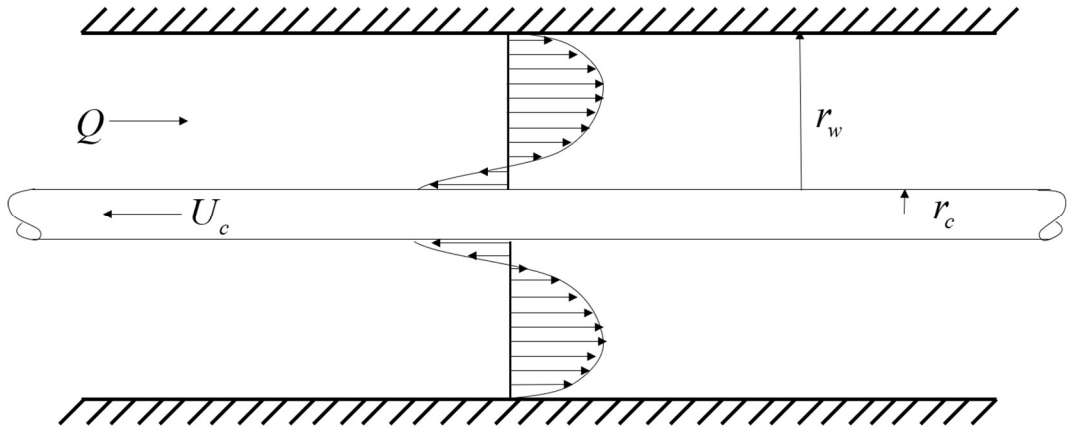

Source: Author (2021)

- Ratio between well and pipe or bit diameter (X)

$$X = \frac{d_w}{d_c} \tag{3.11}$$

The Reynolds number calculated for the drill bit annular spaces are shown in Table 3 and Table 4. The Reynolds number reaches a turbulent regime (Re>2400) in the annular space of the drill bit for water when the displacement speed of the drill string is of 10 cm/s and the cuttings bed is filling 50% of the well. This happens due to the small annular area that the fluid has to flow as the cuttings bed is growing. The

higher the cuttings bed, the higher is the Reynolds number. For the 1 cm/s displacement speed the flow stays in laminar regime in all cases, as well as for the glucose syrup solution, which are laminar due to the fluid higher viscosity (65 times the water viscosity).

Table 3. Reynolds number for water at the drill bit annular space

Water	23.6%	35.7%	50%
1 cm/s	150	191	458
10 cm/s	1508	1913	4585

Source: Author (2021)

Table 4. Reynolds number for glucose syrup solution at the drill bit annular space

Glucose syrup	23.6%	35.7%	50%
1 cm/s	2	3	7
10 cm/s	23	29	70

Source: Author (2021)

While Table 5 and Table 6 show the results for the Reynolds number for the drill string annular space for water and glucose syrup solution. Different from the drill bit annular space, the Reynolds number is in laminar regime for all cuttings bed initial heights.

Table 5. Reynolds number for water at the drill string annular space

Water	23.6%	35.7%	50%
1 cm/s	40	90	170
10 cm/s	396	898	1697

Source: Author (2021)

Table 6. Reynolds number for glucose syrup solution at the drill string annular space

Glucose syrup	23.6%	35.7%	50%
1 cm/s	0.6	1	8

10 cm/s	6	13	83

Source: Author (2021)

The Reynolds number is seen in the Buckingham Pi Theorem (APPENDIX), for both group of variables, eq. 3.12 and 3.13. For the variables related to the viscous forces the Reynolds number appears for the fluid and particle density, for the inertia forces it is related to the fluid density only.

$$\frac{F_d}{U_c.h.\mu_f} = f\left(\frac{\rho_f.h.U_c}{\mu_f}, \frac{\rho_p.h.U_c}{\mu_f}\right) \tag{3.12}$$

$$\frac{F_d}{U_c^2.h^2.\rho_f} = f\left(\frac{\mu_f}{\rho_f.h.U_c}\right) \tag{3.13}$$

The goal would be relating the dimensionless drag force with the Reynolds number to verify if the force level for different scenarios of pipe displacement speed, cuttings bed height, fluid viscosity and density. Both dimensionless drag force and Reynolds number are great in helping the understanding of each variable influence on the pipe displacement and hill and plug formation, however, due to the variables chosen to perform the experiments in this work these relations are not possible. Each parameter that is altered completely changes the conditions. For instance, changing the displacement speed from 1 to 10 cm/s, changes the Reynolds number by ten times, while changing the fluid viscosity the change goes to approximately 65 times, since the viscosity used is 1 and 65 cP.

4 RESULTS

In this chapter, the experimental results are presented and discussed. The results are divided by working fluids and the influence of displacement speed, rotation and cuttings bed height. All tests results were performed three times in order to have a solid force reading.

4.1 Test results description

Firstly, the experimental rig was tested in order to verify its repeatability. The test was performed on a 33 mm cuttings bed height, which represents 23.6% of the cross-sectional area of the wellbore, at 10 cm/s axial displacement speed without rotation. Two tests were performed at the same condition and the results are shown in Figure 17. The force values required to remove the column from the wellbore were very similar for both tests, demonstrating good repeatability. The cuttings movement was also quite similar. The hill formed at end of the test is shown in Figure 18.

In the beginning of every test, the apparatus shows a drag force increase due to the inertia. To seal the upper part of the well, the drill pipe is attached to a flange-gasket set. While the column is displaced in and out the acrylic pipe, the fluid is contained at the gasket. The gasket causes an additional drag load as the pipe accelerates. This initial force increment is observed in all the tests as shown in Figure 17 in the beginning of the test, from $t \sim 0s$ to $t \sim 0.5s$. Additionally, the force increases due to the initial contact between the drill bit and the cuttings bed and the cuttings-cuttings contact, where the cuttings start forming the hill, as also depicted in Figure 17 from $t \sim 0.5s$ to $t \sim 2s$. Which is followed by a slightly decrease once the cuttings are arranged in the hill, keeping a constant force level. In some tests, however, this increment is not well evident in the force readings due to the high pipe speed and pipe rotation.

Figure 17. Axial measured force for a 33 mm (23.6% of the well's height) cuttings bed height at 10 cm/s displacement speed without rotation. This figure shows the results for two tests at the same conditions.

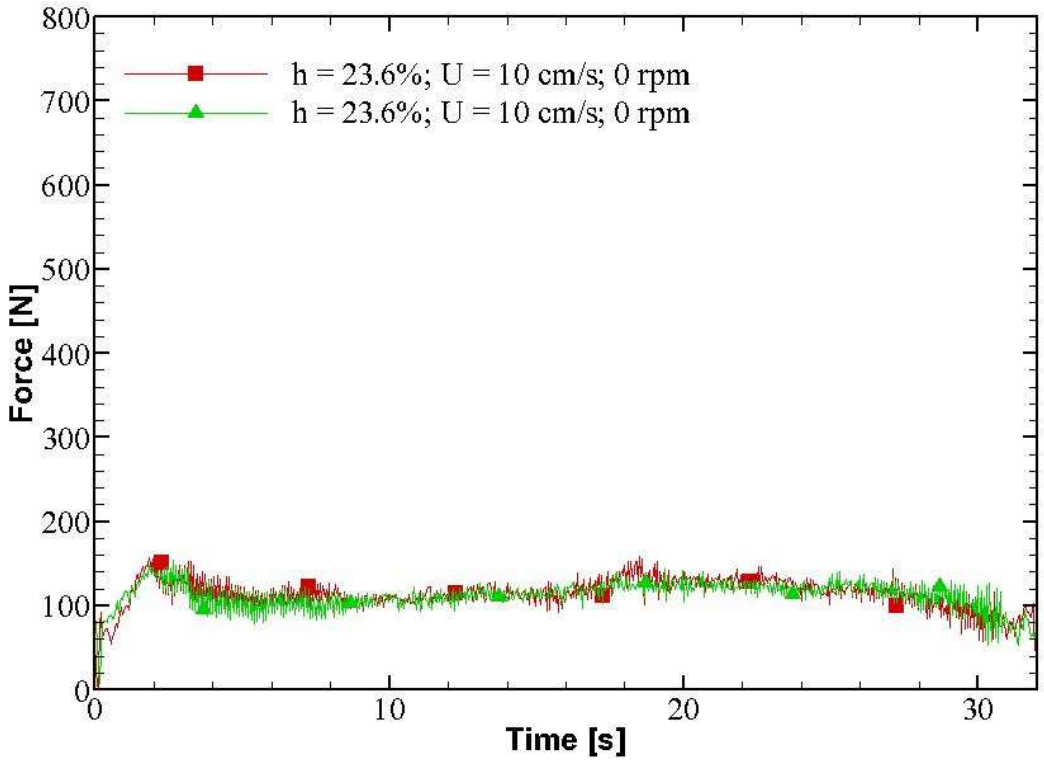

Source: Author (2021)

Figure 18. Cuttings hill formed after displacing the column to the left with a 33 mm (23.6%) cuttings bed height at 10 cm/s displacement speed without rotation. The hill reached 20 cm long.

Source: Author (2021)

The drag force is almost constant throughout the pipe removal for the result showed in Figure 17. This was one of the cases also seen by Rasi (1994) and Peliano (2018), in which the amount of cuttings being carried through the annular space is balanced by the cuttings volume that is incorporated to the hill behind the drill bit.

4.1.1 Tests with water as the working fluid

In this section, water at room temperature was used as the working fluid with viscosity of 1 cP. The results show the influence of axial displacement speed, rotation and cuttings bed height. Figure 19 shows the result for a test with an axial displacement speed of 1 cm/s, without rotation and cuttings bed height of 70 mm (50% of the well diameter). It is observed that the force increases exponentially, which is the result of a hill of cuttings that accumulates continuously behind the drill bit forming a plug. The plug, depicted in Figure 20, reaches a length of 0.98 m fastening the pipe to the well. In such condition, the apparatus force limit is found within the drill string displacement path that takes place at $t \sim 250s$. This exponential force growth was also reported by Rasi (1994).

Figure 19. Axial measured force for a 70 mm cuttings bed height (50% of the well's diameter) at a displacement of 1 cm/s, without rotation.

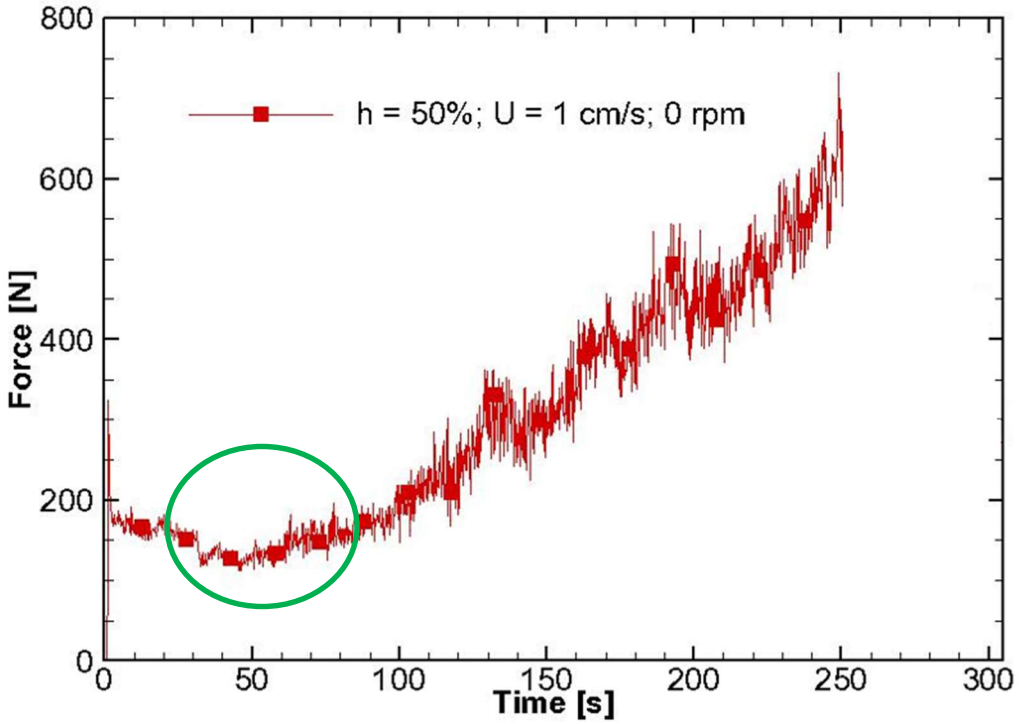

Source: Author (2021)

Figure 20. Plug formed after displacing the drill pipe to the right for the 70 mm cuttings bed height, with pipe displacement speed of 1 cm/s without rotation. The plug reached 98 cm long.

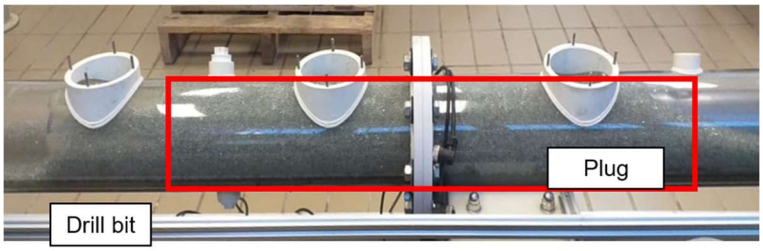

Source: Author (2021)

In the beginning of the test, the drag force shown in Figure 19 overshoots due to the inertia of the apparatus caused by the gasket and by the cuttings bed. Soon after, the force declines slowly, as indicated by the green circle, to start growing again after 50s. The slow force reduction occurs because the hill of cuttings formed behind the drill bit is rearranged and start to fill the drill bit grooves. Since the fluid flow for this particular test is not capable of carrying the cuttings through the grooves to the drill bit front, the cuttings begin to accumulate behind the drill bit. As the volume of cuttings increase behind the bit, a plug is formed, in which the length grows continuously, leading to a steady force increase after 50s, and finally fasten the pipe to the well.

However, the pipe never gets stuck when the cuttings bed height was lower (23.6% and 35.7%). Although the plug is formed and the force also grows exponentially, the test was performed to the end of the apparatus displacement length. As pictured in Figure 21, the formed plug is considerably smaller than the previous one at 23.6% cuttings bed height.

Figure 21. Plug formed after displacing the drill pipe to the right for the 33 mm cuttings bed height with a pipe displacement speed of 1 cm/s without pipe rotation. The plug reached 35 cm long.

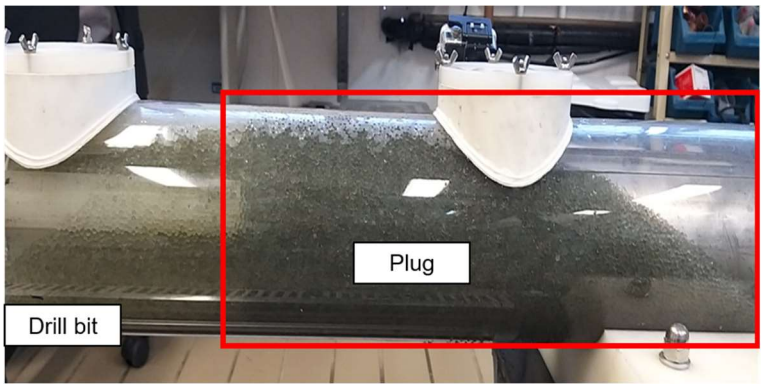

Source: Author (2021)

The results obtained for the pipe displacement at 1 cm/s without rotation are in accordance with the experimental works reported in the literature as well as the granular media studies. The amount of cuttings in the well has a critical influence on the stuck pipe situation. For the experiment's conditions, the pipe gets stuck when the wellbore is filled with 50% of its cross-sectional area with cuttings. However, a cleaner well (35.7% or less of its cross-sectional area) does not cause problems to the pipe displacement. This relation of cuttings bed initial height may be evaluated by comparing the drill bit area and the area above the cuttings bed, as proposed by Rasi (1994). Rasi (1994) observed that if the drill bit area is smaller than the area above the cuttings bed a plug is not formed with the hill maintaining a constant volume during the displacement. On the other hand, a continuous hill growth, followed by a plug formation and, consequently, a stuck pipe occurs if the bit area is larger than the area above the cuttings bed. For the conditions presented in current work, the drill bit area is larger than the area above the cuttings bed in all cases.

Additionally to the fact that the plug was formed for the smaller cuttings bed height, there was a tendency for plug formation with an eventual stuck pipe condition if the pipe were displaced for a longer path. Which means that displacing the drill string in really low speed corroborated to accumulate cuttings into the hill, forming the plug.

Although the less amount of cuttings in the wellbore avoids the stuck pipe problem for the test conditions, mainly the pipe length, an alternative to reach a satisfactory result in a 50% filled well was the pipe displacement speed increase. The axial displacement speed was set to 10 cm/s, while the other parameters were kept

and the result for the test is shown in Figure 22. Differently from the 1 cm/s displacement speed case, the cuttings are carried from the back to the front side of the drill bit, forming a hill of cuttings behind the drill bit and keeping a constant height. The force is maintained almost constant and the pipe does not get stuck.

Figure 22. Axial measured force for a 70 mm cuttings bed height (50% of the well's diameter) and displacement speed of 10 cm/s, without rotation and water as the working fluid.

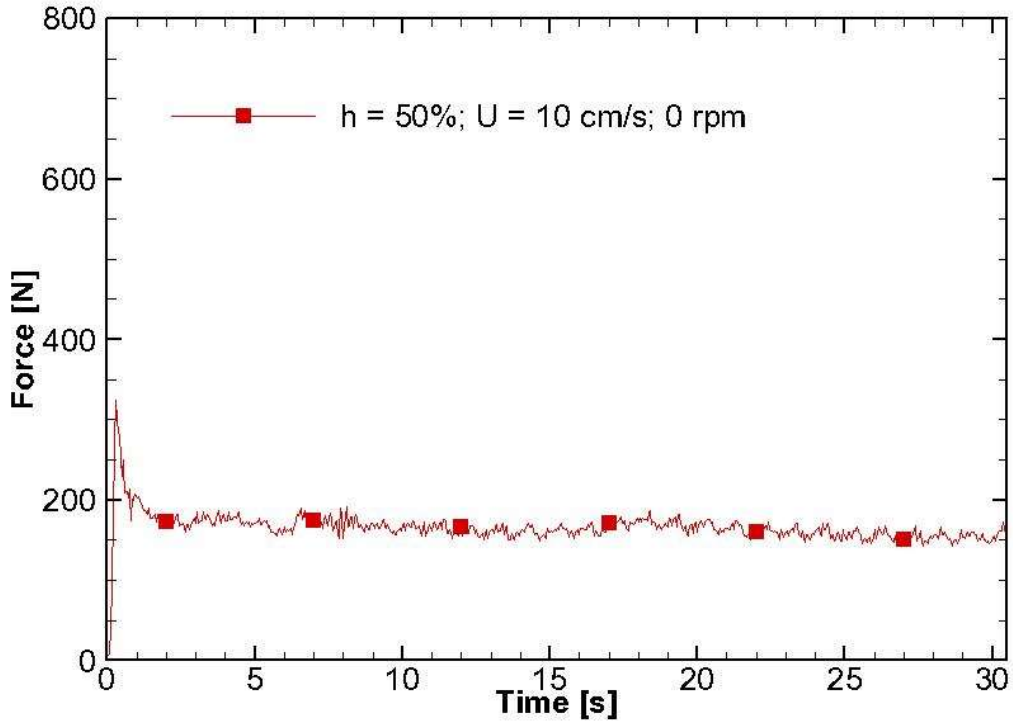

Source: Author (2021)

Common to all tests, the test start-up shows a force increase due to inertia from the apparatus and the cuttings bed. As the increase of the displacement speed creates a scenario where the hill behind the drill bit is constant (the amount of cuttings added to the hill is the same that is carried to the front of the drill bit), the drag force level drops slightly during the pipe displacement path. This cuttings movement is illustrated in Figure 23, where the red arrow indicates the direction of the pipe displacement, while the green arrows indicate the cuttings carried through the drill bit grooves.

Figure 23. Cuttings being carried through the annular space and drill bit grooves from the back to the front of the drill bit. The green arrows indicate the cuttings direction while the red arrow shows the drill string displacement direction.

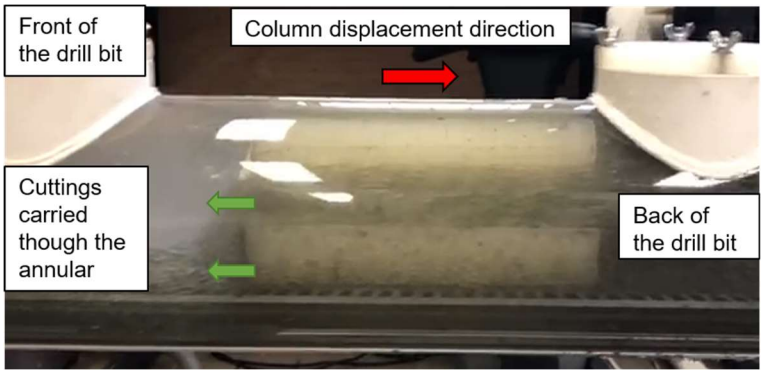

Source: Author (2021)

When comparing this result with Rasi's (1994) statement, it is observed that the relation of drill bit area and open area above the cuttings bed is not the only condition that determine the stuck pipe condition. The drill bit geometry and pipe displacement speed used in this work, for instance, provided different results for the same area relation. The drill bit geometry allowed the cuttings to be carried through its grooves, which was observed for 10 cm/s pipe speed condition.

In addition to the cleaner well, the fluid flow speed increase was also effective preventing the pipe to get stuck. Both results are in accordance with the literature review presented in this work. In cases where the displacement speed could not be increased, an alternative to avoid the stuck pipe could be adding rotation to the column during the displacement. The procedure is similar to a technique called backreaming, in which the fluid is pumped through the annular space while removing and rotating the column (Yarim et al., 2010; Agostini and Nicoletti, 2014; Samuel and Mirani, 2015), as shown in Figure 24. In the current apparatus, it is not possible to pump fluid through the column, however it is possible to rotate the pipe while removing it.

Figure 24. Backreaming process representation. The fluid is pumped though the column (in the direction of the blue arrow) returning through the annular space, while the drillstring is displaced backwards (in the direction of the red arrow) and rotated.

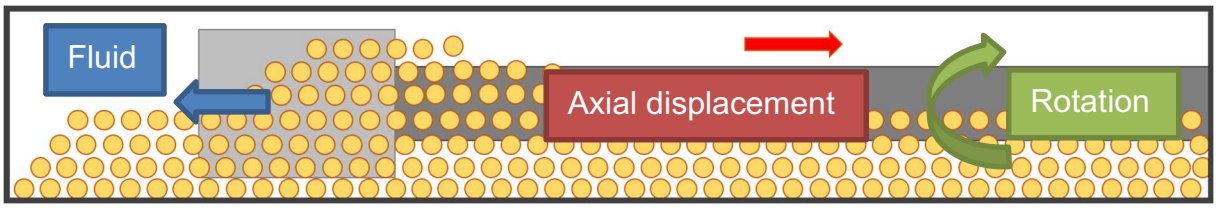

Source: Author (2021)

The previous tests conditions were repeated adding rotation at 25 rpm to the pipe. The results for 1 and 10 cm/s displacement speeds are shown in Figure 25. The drag force for the 1 cm/s displacement speed was completely different from the counterpart case without rotation. Due to the column rotation, the force exponential growth and plug formation were not experienced.

The rotation resulted in a significant reduction of the drag force for both displacement speeds. Additionally, rotation changes completely the test results - the plug is not formed, the hill maintains the same height during the total pipe displacement and consequently, the force is kept in constant levels during the whole test.

Figure 25. Axial measured force for the 70 mm cuttings bed (50% of the well's height) with 25 rpm. The red line with diamonds represents the test at 10 cm/s axial displacement speed, while the blue line with circles indicates the test at 1 cm/s. Both with water as the working fluid.

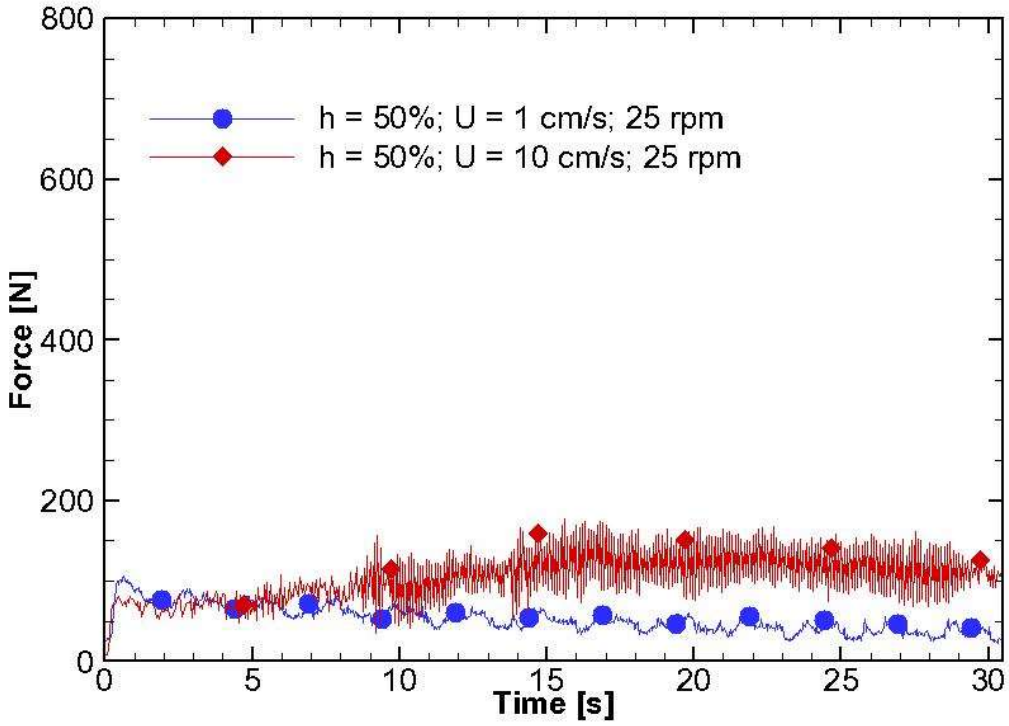

Source: Author (2021)

During the pipe rotation, the edges of the drill bit grooves lift the cuttings bed, moving the particles from the bottom to the top of the horizontal hole, as shown in Figure 26. The suspended cuttings are easier to be carried by the fluid, transferring the cuttings from behind to the front of the drill bit, as depicted in Figure 27. It is worth noting that the pipe rotation not only reduced the drag force but also avoided the pipe being stuck for all cuttings bed height and axial displacement speed.

Figure 26. Representation of the cuttings bed lift by rotating the drill bit. This movement helps the fluid flow to carry the cuttings to the front of the drill bit, avoiding the plug formation.

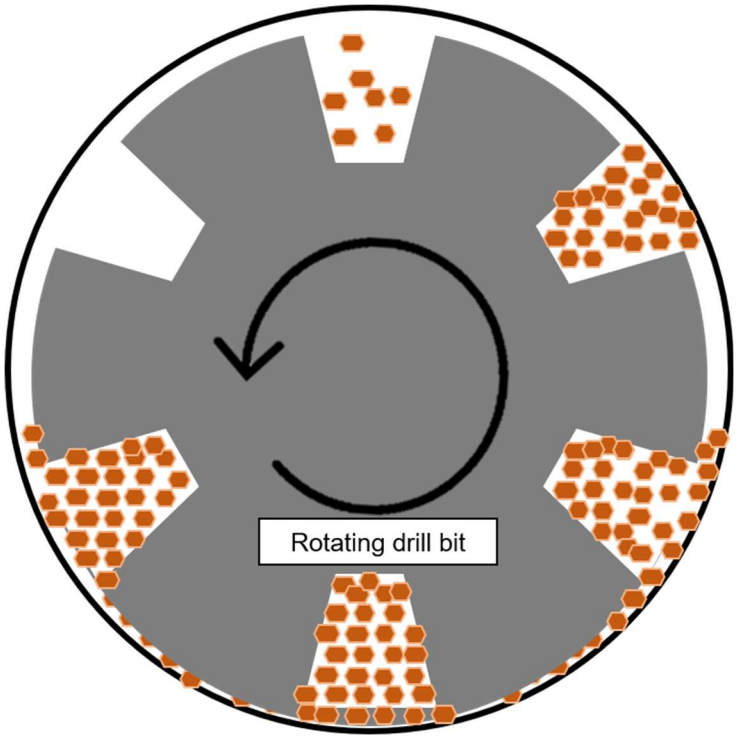

Source: Author (2021)

Figure 27. Cuttings being carried through the annular space and through the drill bit grooves from the back to the front of the drill bit. The green arrows indicate the direction of the cuttings motion, the red arrow shows the drill string displacement direction and the white arrow shows the column rotation.

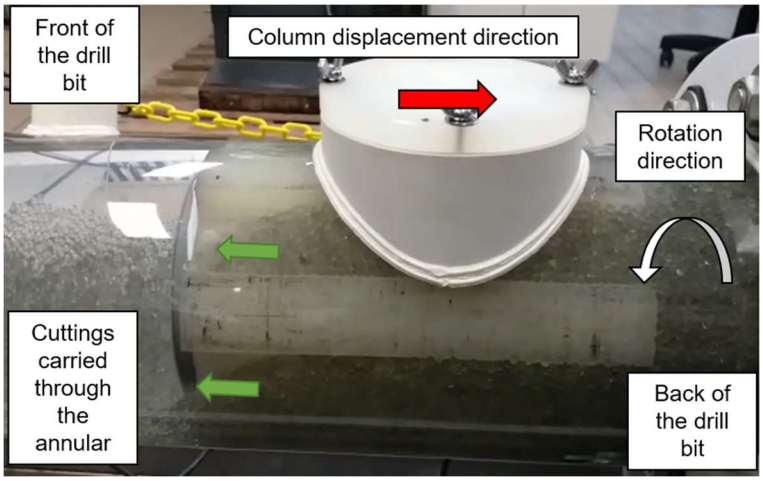

Source: Author (2021)

Different from the work of Knesebeck (2018), the pipe rotation helped avoiding the plug formation. His work, however, was performed by using a drill bit with a larger cross-sectional area, without grooves. There were no grooves to break the cuttings bed structure and move the cuttings from the bottom to the upper part of the well, helping them to be carried to the front of the drill bit.

4.1.2 Tests with glucose syrup solution as the working fluid

This section discusses the results of tests performed with the glucose syrup solution with a viscosity of 65 cP and density of 1.2 g/cm³ at room temperature. The influence of the cuttings bed height, displacement speed and rotation of the drill string is analyzed.

The tests also show an initial drag force due to the apparatus inertia and the cuttings bed. Differently from the tests with water at low displacement speed and without rotation, the current case depicts different force levels, as noted in Figure 28.

Figure 28. Axial measured force for a 70 mm cuttings bed height (50% of the well's diameter) at a displacement speed of 1 cm/s. The red line with squares represents the test without rotation, while the blue line with circles represents the test with rotation at 25 rpm. Glucose syrup solution at 65 cP and 1.2 g/cm³ is the working fluid.

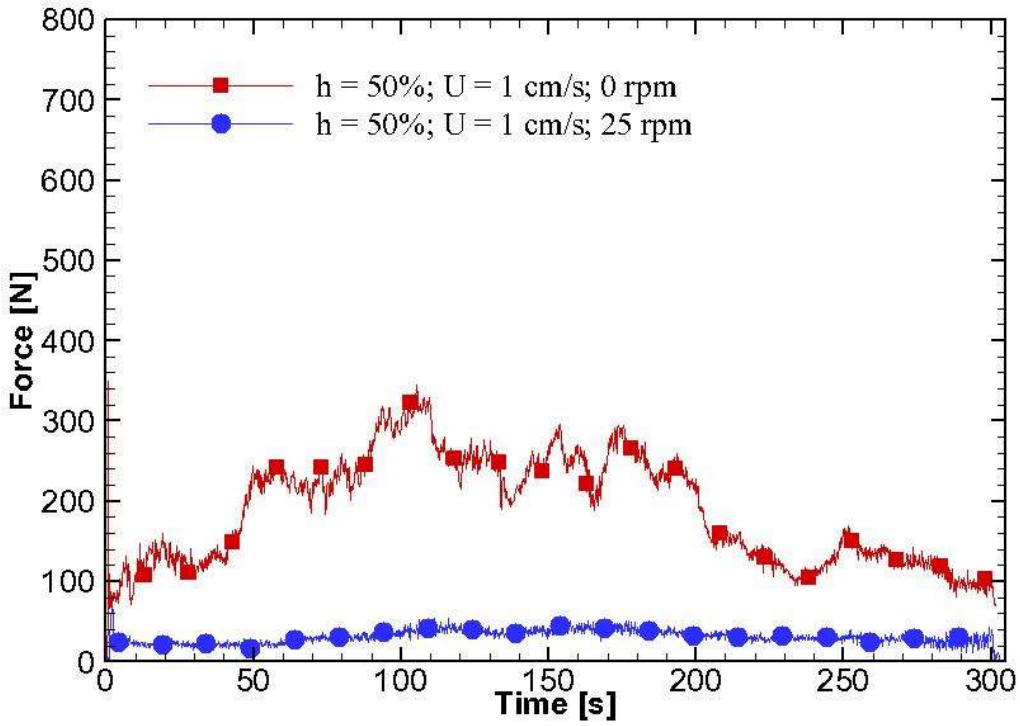

Source: Author (2021)

By comparing the results of Figure 19 with those of Figure 28, one can note that not only the drag force is smaller but also the pipe does not get stuck for the critical condition of 1 cm/s without rotation for a 50% filled cross-sectional area. The smaller level of force measured with glucose can be explained by the higher fluid viscosity and density that provides higher carrying over the cuttings, transporting more particles even for low displacement speeds. According to the literature, by increasing the fluid viscosity the capability of laminar flows of carrying particles increases (Piroozian et al. 2012).

Although the cuttings carrying capability increases, the drill bit geometry causes a force increase at the portion without grooves during the pipe displacement. It is seen in Figure 28 for the test without rotation (red line with squares) that the drag force has different levels. The fluid is able to carry the cuttings through the grooves of the drill bit, however, when the cuttings hit the filled portion of the drill bit, the hill height increases, increasing also the drag force. While the cuttings are being carried through

the grooves, the force keeps the same level, however, when the hill increases, the force level also increases. In Figure 29 it is possible to visualize that the cuttings only pass to the front part of the drill bit between the grooves. So, while the cuttings are passing, the force does not increase, although the hill is increasing a bit in height. When the groove is filled and the cuttings encounter another cog, the force level increases. When the cuttings are being carried through all the grooves, the force level decreases since the fluid is carrying the particles. Thus, the viscosity increase avoids the plug formation as well as the stuck pipe condition. Also, considering Rasi's (1994) area criterion for stuck pipe, the plug and stuck pipe situation did not happen as expected. Differently from water tests, the greater viscosity fluid was able to carry the cuttings despite the drill bit area being larger than the area above the cuttings bed. Therefore, the fluid viscosity should also be taken into account along with the pipe displacement speed.

Figure 29. Cuttings being carried through the grooves of the drill bit. The red arrow shows the pipe displacement direction.

Source: Author (2021)

Although the test without rotation had a completely different behavior when compared to water, adding rotation to this case did not bring any surprise to the results. The force levels, that are shown in Figure 28 in the blue line with circles, were low and the hill showed a continuous length during the pipe displacement, as for the water cases.

The results for the displacement speed of 10 cm/s with and without rotation are shown in Figure 30. Both cases resulted in higher transport of cuttings, reducing the cuttings hill height and, consequently, the force level. The reading noise observed

in the graph is due to the high displacement of the column and is increased even more for the rotating case.

Figure 30. Axial measured force for a 70 mm cuttings bed height (50% of the well's diameter) at a displacement speed of 10 cm/s. The red line with squares represents the test without rotation, while the blue line with circles represents the test with a rotation of 25 rpm. Glucose syrup solution at 65 cP is the working fluid.

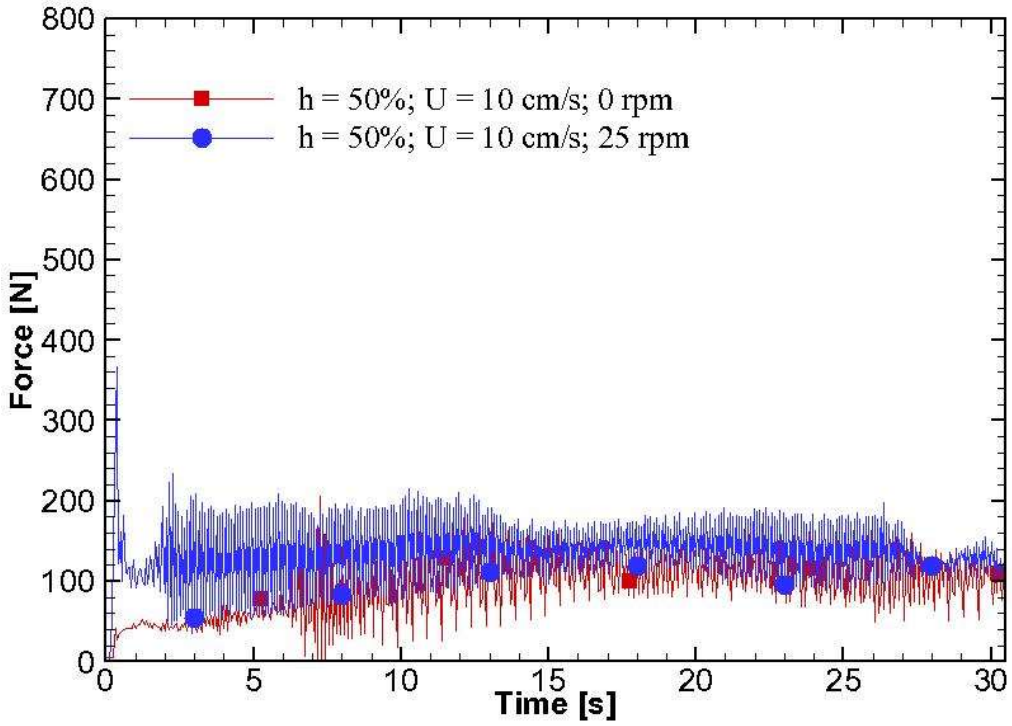

Source: Author (2021)

In summary, none of tests using the glucose syrup solution resulted in a pipe being stuck. This result is mainly due to the greater capability of cuttings being carried in a laminar flow by a more viscous and denser fluid. As expected, for the higher pipe displacement speed and rotation the stuck pipe was also not experienced, being in accordance to the water tests results.

4.1.3 Tests synthesis for hill, plug and stuck pipe scenarios

Gathering all the results it is important to note that a critical case was presented, in which the pipe got stuck for water as the working fluid on a 50% cuttings bed height at 1 cm/s displacement speed without rotation. The results for all

combinations are shown in Table 7 for water and in Table 8 for the glucose syrup solution.

Table 7. Tests results synthesis for water as working fluid

Displacement speed [cm/s]	Rotation [rpm]	23.6%	35.7%	50%
1	0	Plug	Plug	Stuck pipe
1	25	Hill	Hill	Hill
10	0	Hill	Hill	Hill
10	25	Hill	Hill	Hill

Source: Author (2021)

Table 8. Tests results synthesis for glucose syrup solution as working fluid

Displacement speed [cm/s]	Rotation [rpm]	23.6%	35.7%	50%
1	0	Hill	Hill	Plug
1	25	Hill	Hill	Hill
10	0	Hill	Hill	Hill
10	25	Hill	Hill	Hill

Source: Author (2021)

Therefore, slow displacement speeds may cause the increase of the hill behind the drill bit and form a plug, which may cause the stuck pipe condition. However, three solutions were found to avoid the problem in the current work's conditions: displacement speed increase, rotation associated with the drill bit geometry and using a more viscous fluid.

4.2 Shields number

The fluid flow velocity through the annular space increases with the pipe displacement speed. According to the literature review discussed in chapter 2, the greater the flow higher is the transport of cuttings. Nevertheless, the shear stress on top of the particle for compact beds must be larger than that for loose beds. A dimensionless number, called Shields number, can be calculated in order to define

whether the particle would be carried by the fluid flow or not. The Shields number, which is a function of the shear stress on top of a particle, is proposed by Ouriemi's et al. (2007). In their work scenario, a glass pipe filled with a particle bed was used to perform the experiments, the bed surface was considered as a uniform cross-sectional area.

Despite being different, their conditions can be approximated to the current work. There are two cross-sectional areas of interest: the cuttings bed region that is not in contact with the drill bit and the cross-sectional area of the hill. However, in the bed portion that is not in contact with the drill bit, the fluid flow is unable of eroding the bed, which was observed experimentally. As the hill increases, reducing the fluid flow area, the fluid velocity increases. This reduction is caused by the drill bit area and the hill formation that are depicted in Figure 31. Considering the cases evaluated in the current work, the flow would be above the critical Shields number for the portion of cuttings near the drill bit and for the hill's crest.

Figure 31. Cuttings being carried by the fluid flow from the back to the front of the drill bit. The black arrow indicates where the fluid velocity increases due to the reduction on the annular space caused by the drill bit and the hill of cuttings.

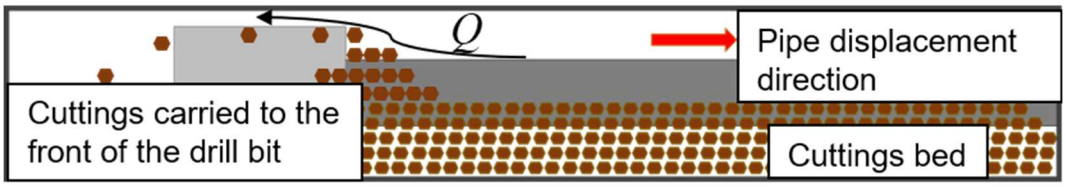

Source: Author (2021)

The Shields number is a dimensionless number defined as the ratio between the shear stress and the particle apparent weight. The Shields number was computed in order to verify a condition where the cuttings would be carried by the fluid flow. The goal was to find a critical number that defines whether the particle would be carried or not.

The calculation was based on Ouriemi et al. (2007) where the authors calculated a critical Shields number for a laminar flow on a particle bed in a glass pipe. In order to calculate the Shields number, θ, the shear rate, $\dot{\gamma}$ (eq. 4.1), the fluid viscosity, μ, the particle diameter, d_p, and the particle density, ρ_p, are necessary.

The calculation for the shear rate is shown in eq.(4.1), which was numerically obtained by the authors.

$$\dot{\gamma} = 11.1\left(\frac{Q}{d_w{}^3}\right)\left(\frac{d_w}{h_f}\right)^2 \tag{4.1}$$

Where h_f is the fluid height, d_w is the well diameter and Q is the fluid flow. In order to verify if the current work's conditions were within the limits considered by the authors to fit the equations and coefficients used in their work, the fluid shear rate was calculated using the experimental rig well diameter and the fluid heights considered were the height above the initial cuttings bed heights (76.4%, 64.3% and 50% of the well height) and a hill formation, which would leave 35.7% of the total well height for the fluid. The current work's conditions show a similar dependence as Ouriemi et al. (2007) work, fitting within the limits of the normalized fluid height of 0.2 to 0.8 which are applied for the shear rate equation, shown in Figure 32.

Figure 32. Curve obtained by normalizing the fluid height by the hole diameter. The slope is in accordance to Ouriemi et al. (2007) work.

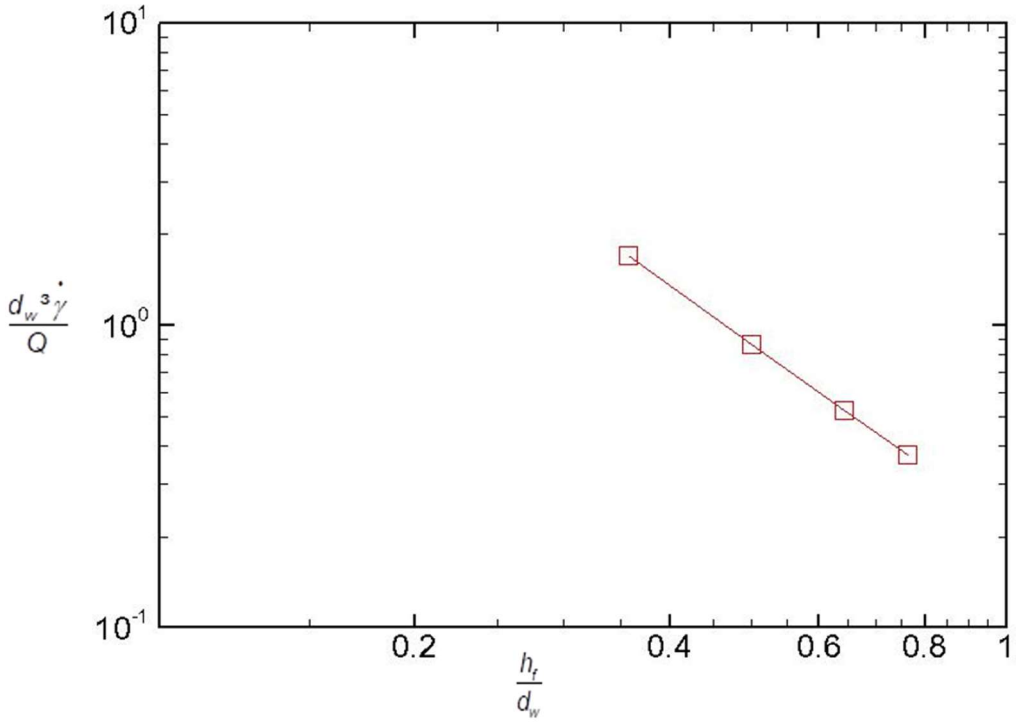

Source: Author (2021)

So, the Shields number is calculated by the eq. (4.2).

$$\theta = \frac{\mu_f \dot{\gamma}}{(\rho_p - \rho_f) d_p g} \tag{4.2}$$

The calculation was performed for water and glucose syrup solution at 1 and 10 cm/s drill string displacement speed, without rotation for five different cuttings heights. Which considers the three initial cuttings bed height used in the present work, and two hill heights were added to consider the hill's growth during the displacement of the drill string for the tests, where the fluid height would be 35.7% and 7.2% of the total well height. The heights used in the calculation are shown in Figure 33.

Figure 33. Hill heights representation used for the Shields number calculation. The percentages are referent to the fluid height above the cuttings and the red line indicates the limit of the cuttings height.

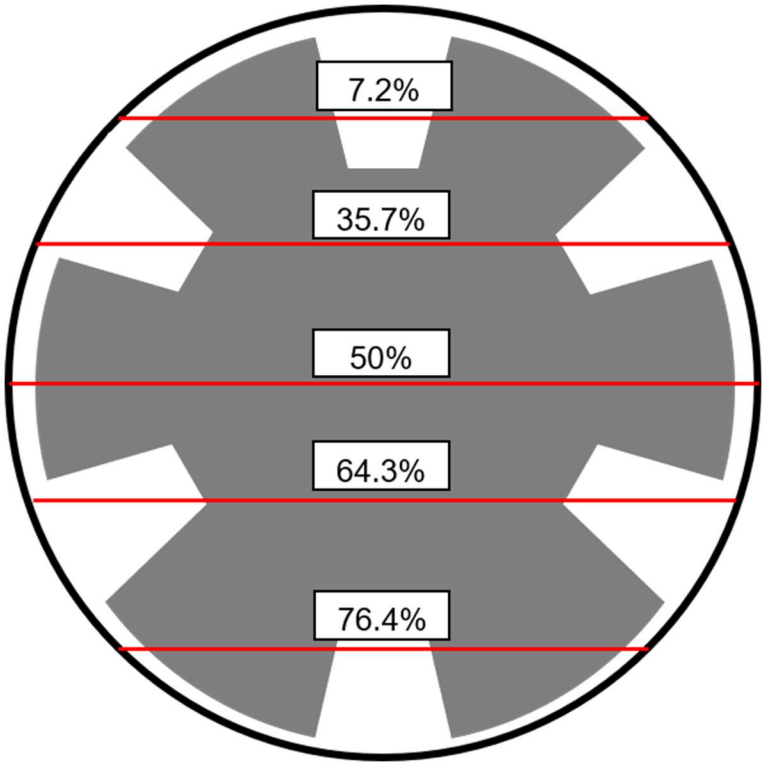

Source: Author (2021)

In order to find out the Shields number that defines the limit whether the particles are carried or not, the video recordings of the tests were analyzed. The analysis of the imagens made possible to estimate the cuttings hill height in which the particles started to be carried. This value was defined as the critical height for each combination of fluid and displacement speed. Since there was no scale on the images, the only way to estimate the height was to use the initial cuttings bed height as a reference.

It was calculated the possible critical Shields number for each combination with the height that the particles began to be carried. According to the estimative, the smaller Shields number that allowed particle carrying was for a displacement speed of 10 cm/s with water as the working fluid at 35.7% fluid height. This value of 10^{-4} was defined as the critical Shields number. In Figure 34 this critical limit is represented by the red line, which imposes that values above it would experience particle transportation by the fluid flow and values below it there would be no bed erosion. Besides, the values calculated for all fluid heights (76.4%, 64.3%, 50%, 35.7% and

7.2% of the total well height) are plotted for each combination of fluid viscosity and column displacement speed.

Figure 34. Shields number calculated for five different cuttings bed height for glucose and water at 1 and 10 cm/s displacement speed. The red line is the limit in which all values above it the particle would be carried, and below it there would be no cuttigs carrying.

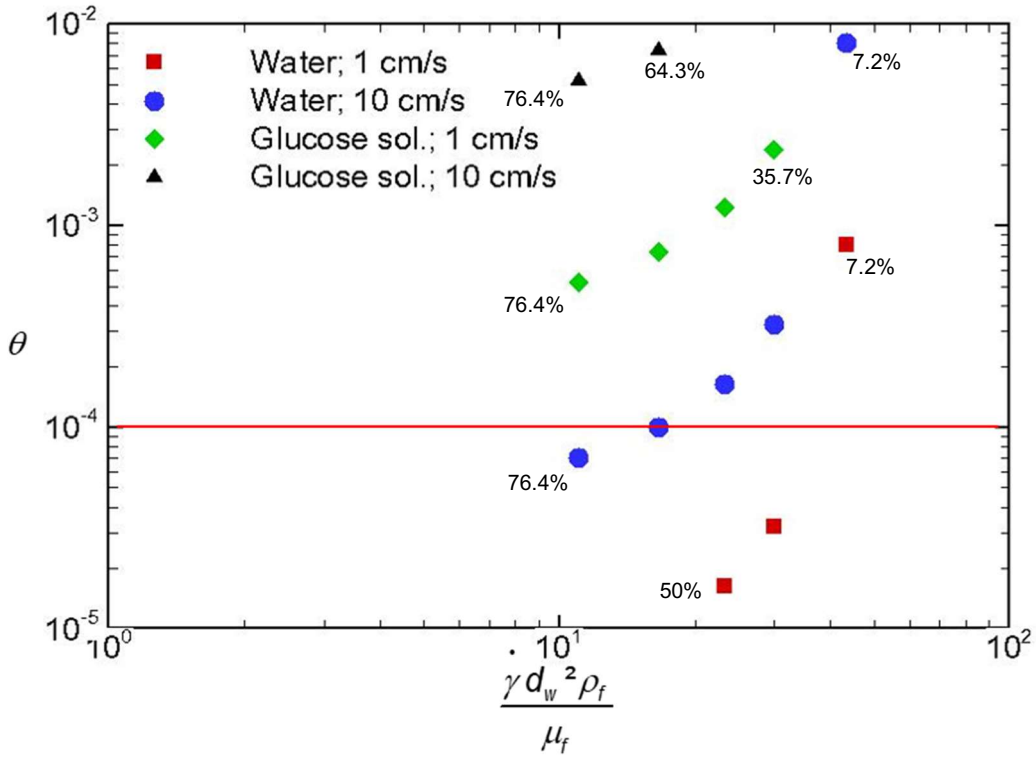

Source: Author (2021)

It is observed that the smaller the area for the fluid to flow through the annular space, the higher is the Shields number, which is caused by the fluid velocity increase. Also, for the higher viscosity fluid (green diamonds and black triangles) the calculated Shields number is above the critical case for the conducted study. It is noted that for the water at 10 cm/s displacement speed, the Shields number for the 76.4% fluid height is the only under the critical limit. While at 1 cm/s displacement speed, despite the 7.2% (which is an almost plug condition), all cases are under it. As for the critical value, the condition is water with a displacement of 10 cm/s at 64.3% fluid height.

The values found by the calculation are in accordance with the experimental results, it was possible to visualize the particle carrying for the cases above the critical Shields number. For the stuck pipe case presented previously in this work of the plug formation, according to the Shields number the only fluid height that the cuttings would

be carried by the fluid flow is the 7.2%. It would require cuttings occupying 92.8% of the cross-sectional area of the well. As the displacement speed is increased, for instance the same condition of initial 50% cuttings bed height, the Shields number is already above the critical value. Which is also in accordance to the results, since the cuttings are carried to the front of the drill bit avoiding the plug formation. In Table 9 and Table 10 a summary of the conditions for cuttings that are carried, which means that the Shields number is above the critical value, is presented.

Table 9. Summary of conditions for cuttings carrying by the fluid flow with water

Water	76.4%	64.3%	50%	35.7%	7.2%
1 cm/s	No	No	No	No	Yes
10 cm/s	No	Yes	Yes	Yes	Yes

Source: Author (2021)

Table 10. Summary of conditions for cuttings carrying by the fluid flow with glucose syrup solution

Glucose syrup	76.4%	64.3%	50%	35.7%	7.2%
1 cm/s	Yes	Yes	Yes	Yes	Yes
10 cm/s	Yes	Yes	Yes	Yes	Yes

Source: Author (2021)

Using the glucose syrup solution as the working fluid there was no plug formation, the cuttings were carried in all tested cases due to the higher viscosity of the fluid. Which is also confirmed by the Shields number calculated being above the critical value for the experiments performed in this work. Even for the critical case of 1 cm/s without rotation, where different force levels were experienced due to the cuttings volume increase behind the drill bit when the particles faced the filled portion of the drill bit, the particles continued to be carried through the grooves since the beginning of the experiment, which is illustrated in **Figure 35**.

Figure 35. The picture of the drill bit shows that the cuttings are only carried through the grooves of the drill bit. Where the edges are near to the hole wall, there is almost no cuttings passage.

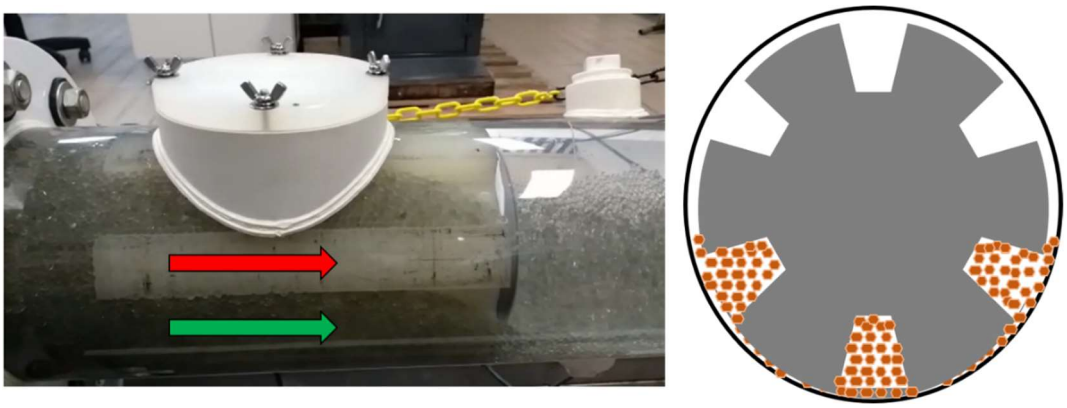

Source: Author (2021)

5 CONCLUSIONS

An experimental rig representing a horizontal well was used to evaluate the T&D caused by interactions between column/drill bit and cuttings bed. In order to reach the objectives, the test parameters were defined and the methodology was developed. The rig's repeatability was observed for the tests performed. Also, using water as the working fluid a stuck pipe condition was experienced. This result was seen for a pipe displacement of 1 cm/s without rotation on a 50% cuttings bed height (70 mm of a 140 mm diameter wellbore). Some solutions in order to avoid the stuck pipe were observed:

i) Having an initial state where the cuttings bed height is smaller avoided the stuck pipe, despite showing an exponential drag force growth and having a plug formation.

ii) Increasing the displacement speed from 1 to 10 cm/s for the same conditions also avoided the stuck pipe due to the greater fluid capability of carrying the cuttings and removing them from behind the drill bit.

iii) For the drill bit geometry used, the rotation was also a solution for removing the cuttings from the bed and helping the fluid to carry the particles in suspension to the front of the drill bit.

iv) Increasing the fluid viscosity from 1 to 65 cP and the density from 1 to 1.2 g/cm³ increased the carrying capability, resulting in more cuttings carried through the annular space of the drill bit, also avoiding the stuck pipe.

By comparing the drill bit area with the open area above the cuttings bed it was observed that more variables should be considered. As presented by Rasi (1994), for the water test at 1 cm/s displacement speed the hill showed a continuous growth as expected by the areas relation. However, the increase in the displacement speed and the greater fluid viscosity changed the scenario. Thus, not only the area relation should be taken into account, but also the drill bit geometry, pipe displacement speed, fluid viscosity and density.

The Buckingham Pi Theorem and Reynolds number were important in order to verify which parameters affect the studied phenomena and to verify that the tests were performed for laminar flow, except for water at 10 cm/s for a cuttings bed higher than 50% of the well's height. However, they could not be used in order to analyze dimensionless drag forces due to the great value differences between the experimental parameters.

The Shields number was calculated to the tested cases and also for two higher hill's heights, where a critical value was defined. It was observed that for values greater than the critical Shields number, the cuttings were carried by the fluid flow. While for smaller values the cuttings were not carried from behind to the front of the drill bit.

5.1 Future works

In order to improve the knowledge that was built in this work and continue the work, it was identified some key points that may be taken into account for future works. Besides the use of the other drill bit model that is available, using different geometry cuttings may have a great impact on the results. Also, using different fluids with distinct viscosity and density is really important. Along the different parameters, the experimental rig may be upgraded using a ball screw with a higher pitch, what would increase the displacement speed range.

These variables may be organized and planned in order to make possible the evaluation using non-dimensional parameters, which was not possible in this work due to the huge parameters' differences. Using parameters that are possible to correlate with Reynolds number and the Buckingham Pi Theorem that was developed may results in great understanding of the phenomena. Therefore, improving the Shields number analysis for the conditions where the cuttings may be carried by the fluid flow.

REFERENCES

Aadnoy BS, Fazaelizadeh M, Hareland G (2010) A 3D analytical model for wellbore friction. J Can Pet Technol 49:25–36.

Agostini CE, Nicoletti R (2014) Lateral vibration of oilwell drillstring during backreaming operation. Proc Int Conf Struct Dyn , EURODYN 2014–Janua:893–898.

Allen B, Kudrolli A (2018) Granular bed consolidation, creep and armoring under subcritical fluid flow. 1610:1–21.

Baratto AC, Damasceno JC, Alves JAP, Filho JT, Couto PRG, Oliveira SP de. (2008) Avaliação de dados de medição — Guia para a expressão de incerteza de medição. <http://www.inmetro.gov.br/noticias/conteudo/iso_gum_versao_site.pdf>.

Coleman HW, Steele WG (2018) Experimentation, Validation, and Uncertainty Analysis for Engineers, Fourth edi.

Costa SS (2006) Modelagem para o Escoamento Transiente Horizontal e Quase Horizontal na Perfuração de Poços de Petróleo.

Cúñez F, Franklin E de M (2019) Experimental Investigation of Liquid-Solid Fluidized Beds in a Narrow Tube.

Fontenot JE, Clark RK (1997) An improved method for calculating swab and surge pressures and circulating pressures in a drilling well. SPE Repr Ser 36–43.

Fox RW, Philip J P, McDonald AT (2015) Introduction to Fluid Mechanics, Nineth edi.

Hambrusch GHL, Negrão COR., Peliano SV, Rosso N de. (2017) Conception and development of an experimental setup for the torque and drag analysis in directional drilling columns.

Hamm E, Tapia F, Melo F (2011) Dynamics of shear bands in a dense granular material forced by a slowly moving rigid body. Phys Rev E - Stat Nonlinear, Soft Matter Phys. doi: 10.1103/PhysRevE.84.041304

Johancsik CA, Friesen DB, Dawson R (1984) Torque and Drag in Directional Wells - Prediction and Measurement. JPT, J Pet Technol 36:987–992.

Knesebeck R (2018) Avaliação experimental do efeito da rotação na força de retirada da coluna de perfuração de um poço horizontal.

Mirhaj SA, Kaarstad E, Aadnoy BS (2016) Torque and drag modeling; Soft-string versus stiff-string models. Proc SPE/IADC Middle East Drill Technol Conf Exhib 2016–Janua:26–28.

Mitchell RF, Samuel R, De H (2007) How Good is the Torque-Drag Model?

Nazari T, Hareland G, Azar J (2010) Review of Cuttings Transport in Directional Well Drilling: Systematic Approach. Proc SPE West Reg Meet. doi: 10.2523/132372-MS

Ouriemi M, Aussillous P, Medale M, Peysson Y, Guazzelli É (2007) Determination of the critical Shields number for particle erosion in laminar flow. Phys Fluids 19:1–5.

Peliano S (2018) Análise experimental do arrasto em colunas de perfuração parcialmente imersas em leito de cascalhos.

Petrobras (2019) Pré-Sal. <http://www.petrobras.com.br/pt/nossas-atividades/areas-de-atuacao/exploracao-e-producao-de-petroleo-e-gas/pre-sal/>. Accessed:10/09/2019.

Petrobras (2014) Fatos e dados - Reduzimos em 55% o tempo de perfuração de poços no pré-sal. <http://www.petrobras.com.br/fatos-e-dados/reduzimos-em-55-o-tempo-de-perfuracao-de-pocos-no-pre-sal.htm>. Accessed:18/11/2019.

Petrobras (2015a) Conheça os diferentes tipos de poços de petróleo e gás natural. <http://www.petrobras.com.br/fatos-e-dados/conheca-os-diferentes-tipos-de-pocos-de-petroleo-e-gas-natural.htm>. Accessed:10/09/2019.

Petrobras (2015b) A descoberta de um campo de petróleo e gás natural em 5 passos. <http://www.petrobras.com.br/fatos-e-dados/a-descoberta-de-um-campo-de-petroleo-e-gas-natural-em-5-passos.htm>. Accessed:10/09/2019.

Piroozian A, Ismail I, Yaacob Z, Babakhani P, Ismail ASI (2012) Impact of drilling fluid viscosity, velocity and hole inclination on cuttings transport in horizontal and highly deviated wells. J Pet Explor Prod Technol 2:149–156.

Rasi M (1994) Hole Cleaning in Large, High-Angle Wellbores. Drill Conf - Proc 299–310.

Rojas S, Ahmed R, Elgaddafi R, George M (2017) Flow of power-law fluid in a partially blocked eccentric annulus. J Pet Sci Eng 157:617–630.

Samuel R, Mirani A (2015) Vibration modeling and analysis under backreaming condition. Proc - SPE Annu Tech Conf Exhib 2015–Janua:1034–1049.

Sheppard MC, Wick C, Burgess T (1987) Designing Well Paths To Reduce Drag and Torque. SPE Drill Eng 2:344–350.

Sifferman TR, Becker TE (1997) Hole cleaning in full-scale inclined wellbores. SPE Repr Ser 16–21.

Tang M, Ahmed R, He S (2016) Modeling of yield-power-law fluid flow in a partially blocked concentric annulus. J Nat Gas Sci Eng 35:555–566.

Tordesillas A, Steer CAH, Walker DM (2014) Force chain and contact cycle evolution in a dense granular material under shallow penetration. Nonlinear Process Geophys 21:505–519.

Wang X, Chen P, Ma T, Liu Y (2017) Modeling and experimental investigations on the drag reduction performance of an axial oscillation tool. J Nat Gas Sci Eng 39:118–132.

White FM (1998) Fluid Mechanics, Fourth edi.

Wiktorski E, Khatibi M, Sui D, Time RW (2018) Study of Frictional Forces Between Rotating Pipe and Wellbore in Horizontal Wells: Experimental and Modeling. 10.

Yarim G, Ritchie GM, May RB (2010) A guide to successful backreaming: Real-time case histories. SPE Drill Complet 25:27–38.

Yarin LP (2012) The Pi-Theorem. Application to Fluid Mechanics and Heat and Mass Transfer.

Zhou L (2008) Hole Cleaning During Underbalanced Drilling in Horizontal and Inclined Wellbore. SPE Drill Complet 23:267–273.

APPENDIX A – Buckingham Pi Theorem

To better understand the torque and drag forces involved in the experiment, the Buckingham Pi theorem was used. This theorem allows simplification of experimental and theoretical analysis (Yarin 2012). The first step is listing all the parameters that may affect the phenomenon. The parameters that have the fundamental dimensions, such as mass, length and time, are then selected. All the other parameters must be listed with respect to the primary parameters. The next step is to form dimensionless equations by combining all the other parameters with the primary ones (White 1998; Fox et al. 2015).

The drag force, F_d, is here assumed to be a function of axial displacement speed, U_c, fluid density, ρ_f, particle density, ρ_p, cuttings bed height, h, rotational speed, Ω, drill bit diameter, d_{db}, column diameter, d_c and well diameter, d_w, particle diameter, d_p, fluid viscosity, μ_f and gravity, g.

$$F_d = f(U_c, \rho_f, \rho_p, h, \Omega, d_{db}, d_c, d_w, d_p, \mu_f, g) \tag{A.1}$$

To find the dimensionless force, Π_1, the F_d must be the first term multiplied by the three primary terms. In the current case, the chosen terms were: the fluid viscosity, cuttings bed height and displacement speed, since they have the mass M, length L and time T units.

$$\begin{aligned}
&\Pi_1 = F_d.U_c^{\,a}.h^b.\mu_f^{\,c} \\
&\Pi_1 = (MLT^{-2}).(LT^{-1})^a.(L)^b.(ML^{-1}T^{-1})^c \\
&a = -1 \\
&b = -1 \\
&c = -1 \\
&\Pi_1 = \frac{F_d}{U_c.h.\mu_f}
\end{aligned} \tag{A.2}$$

Following this methodology for the other terms, one can find the following Π_2 .to Π_9:

$$\Pi_2 = \frac{\Omega.h}{U_c} \tag{A.3}$$

$$\Pi_3 = \frac{\rho_f.h.U_c}{\mu_f} \tag{A.4}$$

$$\Pi_4 = \frac{\rho_p.h.U_c}{\mu_f} \tag{A.5}$$

$$\Pi_5 = \frac{d_{db}}{h} \tag{A.6}$$

$$\Pi_6 = \frac{d_c}{h} \tag{A.7}$$

$$\Pi_7 = \frac{d_w}{h} \tag{A.8}$$

$$\Pi_8 = \frac{d_p}{h} \tag{A.9}$$

$$\Pi_9 = \frac{g.h}{U_c^2} \tag{A.10}$$

Π_1 is then written as a function of Π_n :

$$\Pi_1 = f(\Pi_2, \Pi_3, \Pi_4, \Pi_5, \Pi_6, \Pi_7, \Pi_8, \Pi_9)$$
$$\frac{F_d}{U_c.h.\mu_f} = f\left(\frac{h.\Omega}{U_c}, \frac{\rho_f.h.U_c}{\mu_f}, \frac{\rho_p.h.U_c}{\mu_f}, \frac{d_{db}}{h}, \frac{d_c}{h}, \frac{d_w}{h}, \frac{d_p}{h}, \frac{g.h}{U_c^2}\right) \tag{A.11}$$

A similar result can be obtained for the torque, T:

$$T = f(U_c, \rho_f, \rho_p, h, \Omega, d_{db}, d_c, d_w, d_p, \mu_f, g)$$
$$\frac{T}{h^2.\mu_f} = f\left(\frac{h.\Omega}{U_c}, \frac{\rho_f.h.U_c}{\mu_f}, \frac{\rho_p.h.U_c}{\mu_f}, \frac{d_{db}}{h}, \frac{d_c}{h}, \frac{d_w}{h}, \frac{d_p}{h}, \frac{g.h}{U_c^2}\right) \tag{A.12}$$

For the chosen primary variables, both torque and drag force are functions of Reynolds numbers based on the specific mass of the particle and fluid. By replacing the specific mass by the fluid viscosity as a primary variable, the following dimensionless numbers were found: